

RESEARCH ARTICLE

Critical diversity: Divided or united states of social coordination

Mengsen Zhang^{1*}, J. A. Scott Kelso^{1,2}, Emmanuelle Tognoli¹

1 Center for Complex Systems and Brain Sciences, Florida Atlantic University, Boca Raton, Florida, United States of America, **2** Intelligent System Research Centre, Ulster University, Derry ~ Londonderry, Northern Ireland

* zhang@ccs.fau.edu



OPEN ACCESS

Citation: Zhang M, Kelso JAS, Tognoli E (2018) Critical diversity: Divided or united states of social coordination. PLoS ONE 13(4): e0193843. <https://doi.org/10.1371/journal.pone.0193843>

Editor: Dante R. Chialvo, Consejo Nacional de Investigaciones Científicas y Técnicas, ARGENTINA

Received: January 9, 2018

Accepted: February 6, 2018

Published: April 4, 2018

Copyright: This is an open access article, free of all copyright, and may be freely reproduced, distributed, transmitted, modified, built upon, or otherwise used by anyone for any lawful purpose. The work is made available under the [Creative Commons CCO](#) public domain dedication.

Data Availability Statement: Data are available at DOI [10.1371/journal.pone.0193843](https://doi.org/10.1371/journal.pone.0193843) | ARK [c7605.osf.io/sc9p6](https://doi.org/10.5063/c7605.osf.io/sc9p6).

Funding: This work was supported by the National Institute of Mental Health (MH080838 and EB025819), the Chaire d'Excellence Pierre de Fermat, and the Davimos Family Endowment for Excellence in Science. The funders had no role in study design, data collection and analysis, decision to publish, or preparation of the manuscript.

Competing interests: The authors have declared that no competing interests exist.

Abstract

Much of our knowledge of coordination comes from studies of simple, dyadic systems or systems containing large numbers of components. The huge gap ‘in between’ is seldom addressed, empirically or theoretically. We introduce a new paradigm to study the coordination dynamics of such intermediate-sized ensembles with the goal of identifying key mechanisms of interaction. Rhythmic coordination was studied in ensembles of eight people, with differences in movement frequency (‘diversity’) manipulated within the ensemble. Quantitative change in diversity led to qualitative changes in coordination, a critical value separating régimes of integration and segregation between groups. Metastable and multifrequency coordination between participants enabled communication across segregated groups within the ensemble, without destroying overall order. These novel findings reveal key factors underlying coordination in ensemble sizes previously considered too complicated or ‘messy’ for systematic study and supply future theoretical/computational models with new empirical checkpoints.

Introduction

The function of living systems (e.g. brain, human society, ecosystem) depends on the coordination of multiple components and processes. Such coordination depends on intrinsic characteristics of the interacting entities as well as the form of interaction between them [1–4]. Living systems exhibit a myriad of rhythmic behaviors [5], e.g. humans with their daily, weekly, monthly routines [6] and physiological rhythms [7]; brains with their waves [8]; and species with their life-cycles [9]. By virtue of its temporal symmetry (i.e. translational symmetry in time), rhythmic coordination serves as a fine soil for experimental and theoretical study of laws of interaction between components of dynamical systems. The study of two interacting entities has laid experimental and theoretical foundations for addressing how coordinative structures form, adapt and change. Whether it is humans coordinating with sensory stimuli [10,11], coordinated movements within the same person [12–15], between two persons [16–22], two neuronal populations [23,24], humans and machines [25–27], or humans and other species [28,29], similar tendencies to form or learn certain relative phase and frequency patterns have been observed. Essential phase patterns, their stabilities and transitions have been

well described mathematically in terms of informationally coupled dynamical systems [30–33]. A little beyond dyads, triadic and tetradic coordination have been studied mainly in animal gaits or multilimb movements with a richer repertoire of patterns—combinations of dyadic patterns satisfying certain symmetry constraints [34–38]. Beyond systems with a relatively small number of interacting components, the focus of interest leaps toward systems of much larger scales—e.g. flashing fireflies [39], neuronal populations [40], or the clapping of an ardent audience [41]—whose sheer size eludes detailed investigational techniques but favors low-dimensional measures at coarser scales (e.g. collective synchronization). Such synchronization has been reproduced in various coupled oscillator models, e.g. [42–45].

Despite this gap between systems of very few and very many components (with rare exceptions, [46]), daily social interaction often unfolds in the middle, for example, coordinating with a group of colleagues at work, or afterwards engaging in a variety of gatherings with friends and families, or various forms of folk dancing and Ceilidhs. The choice of the number of independently manipulatable components goes hand in hand with available paradigms for approaching coordination phenomena. With very few components, the repertoire of collective patterns and phase transitions can be fully explored with the help of experimental manipulation and theoretical models, but the limited size may curtail the complexity of spatial organizations. With very many components, possible coordination patterns (described at a microlevel) become too numerous to be studied exhaustively (due to high dimensionality of the phase space); the large number of components also makes it difficult to utilize systematic manipulations to carry the system through its repertoire of possible patterns. Instead, low-dimensional (macro) measures such as the overall level of synchronization can serve as an order parameter to capture collective states of the system [1,43]. As important as such descriptions of coordination are, macro measures meet their limit when one attempts to characterize the system's organizational complexity. Under the broad umbrella of “incoherent” states, what are the possible organizations? How can we explore such organizations systematically in the laboratory? To answer these kinds of questions, a way is needed to experimentally manipulate the system's coordination dynamics on multiple spatial and temporal scales of description. We chose an ensemble of intermediate size ($N = 8$ people) operating under the assumption that this is big enough to reveal the system's organizational complexity, yet small enough to yield to experimental manipulation. Our strategy was to bridge this two-fold gap of system size and experimental control.

We studied rhythmic movement coordination in ensembles of eight people who were predisposed to move at the same or different frequencies. Existing empirical findings and theories suggest that the form and stability of coordination varies with the strength of coupling and the difference in natural frequency (frequency predisposition) between components [11,32,47]. On this basis, we hypothesized that manipulating the distribution of frequency predispositions and coupling strength should produce different propensities for coordination, and induce different forms of collective behavior. Because it is possible to control systematically and measure quantitatively, frequency difference was chosen as a parameter to manipulate diversity within and between group members. We wanted to know how different diversity conditions favor the formation, persistence and change of multiple groups that are potentially integrated within themselves but segregated between each other.

Results

Fifteen independent ensembles of eight people ($N = 120$) participated in the study (for details see [Materials and Methods](#)). All were instructed to tap rhythmically on a touchpad. At the beginning of each trial, members of an ensemble were each paced with a metronome; after the

pacing period, they were able to see each other's taps as flashes (dubbed "human fireflies") on an array of LEDs situated at eye height in front of them. The task was to keep tapping at one's own metronome frequency (tempo) throughout the entire trial. No instructions were given to coordinate with others.

To study how patterns of coordination among participants may form or dissolve, we introduced different levels of diversity by manipulating the assignment of metronomes to each participant. The metronomes divided the participants into two groups of four with frequency difference (δf , also referred to as level of diversity below) of either 0 Hz (1.5 vs. 1.5 Hz), 0.3 Hz (1.35 vs. 1.65 Hz), or 0.6 Hz (1.2 vs. 1.8 Hz). Within each group the four participants were paced at the same frequency. Overall, participants followed the metronome frequency during both pacing and interaction phases, in accord with instructions (see Section E in [S1 File](#)). In the following sections, we demonstrate the main findings, which may be best read along with the extended quantitative and theoretical analyses provided in the Supporting Information ([S1 File](#)).

Spontaneous phase coordination and spatiotemporal metastability

The dynamics of relative phase between participants revealed that the participants spontaneously coordinated in various phase patterns and switched between them, despite not being given any instruction to do so. Such dynamic patterns are exemplified in [Fig 1A1–1A3](#) which shows a trial of interaction among three persons (labeled with numbers 1, 3 and 4, reflecting spatial location on LED arrays, see legends under A2). The evolution of their relations is shown in (A1) as trajectories of dyadic relative phase (ϕ , reported in radians throughout this paper) for pairs 3–4 (orange) and 1–3 (red). When a trajectory is horizontal, the pair is strongly coordinated by holding an (almost) constant phase relation (termed phase locking or dwell); when the trajectory is tilted, the pair is uncoordinated (phase wrapping). Dyad 3–4 (orange) engaged in a long dwell at inphase ($\phi \approx 0$, 10–35s in A1, largest peak in A2), then switched to a near antiphase pattern ($\phi \approx \pi$, 40s onward in A1, small peak in A2). Such near inphase/antiphase patterns are signs of bistability widely observed in biological coordination [48]. Dyad 1–3 (red) also coordinated near inphase but in much briefer and recurrent dwells (around 10, 20, 30s in A1, largest red peak in A2), interleaved with escapes from it. This type of intermittent or relative coordination [49] characterized by consecutive epochs of dwells and escapes corresponds to the metastable regime in models of coordination dynamics [3,50]. Evidence for metastability was often seen in single trial dynamics (see Section J in [S1 File](#) for a statistical approach). Besides bistable and metastable coordination observed within specific pairs of participants, a higher order interaction becomes apparent when we examine the two pairs together: during the long dwell of Dyad 3–4, three epochs of phase shift (bumps in orange curve at 15, 25, 35s in A1) followed precisely after each dwell of Dyad 1–3 (red). Moreover, as each dwell of Dyad 1–3 became longer than the previous one, the phase shift in Dyad 3–4 became bigger, to the point where the shift was so big (38s) that Dyad 3–4 broke up their predominant inphase pattern and switched to antiphase. This finding indicates that the joining of a new member (e.g. person 1) induced changes in preexisting coordinative relations (e.g. Dyad 3–4), strongly suggesting that multiagent coordination is more than the sum of isolated dyads (see Section H in [S1 File](#) for a statistical analysis). As an aid to visualization, the spatial arrangement corresponding to the foregoing temporal changes are illustrated in A3.

In the experiment, epochs of phase coordination were mostly transient or intermittent (i.e. metastable dwells), covering a wide range of time scales, with a mean duration of 4.64s ($\pm 4.04s$) and a long tail of more persistent phase patterns up to the entire duration of interaction, about 50s (See Fig B in [S1 File](#) for distribution). The confluence of metastability and multiple

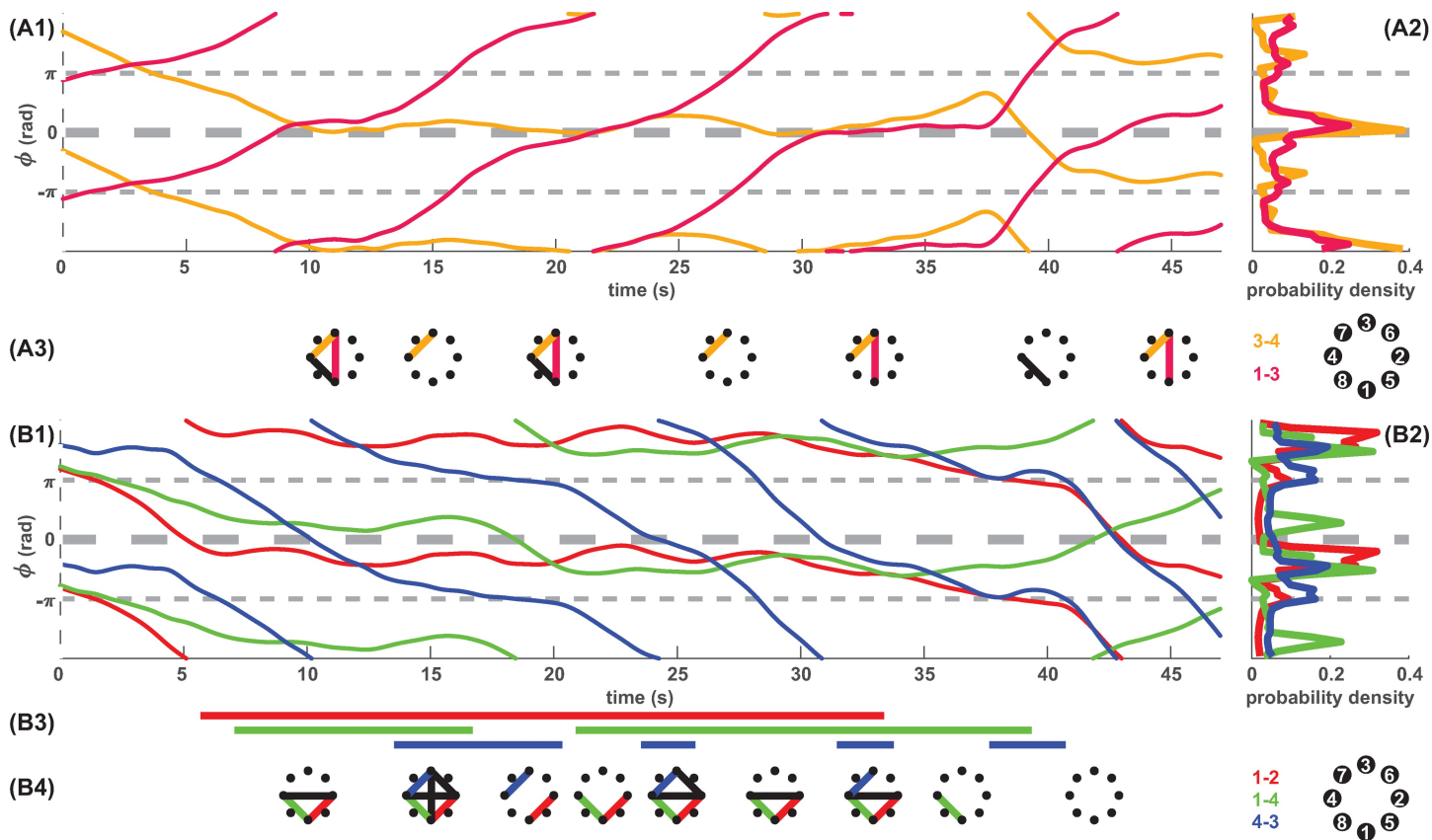


Fig 1. Coordination dynamics of phase relations among multiple agents. (A1) Exemplary relative phase trajectories show the metastable phase coordination of three persons (2 moduli plotted to help perceiving trajectories' temporal continuity). Shortly into the interaction stage (10s), dyad 3–4 coordinated near inphase for 25s (relative phase $\phi \approx 0$ orange, flattening of ϕ trajectories indicates phase coordination, or dwells), then switched into a pattern near antiphase ($\phi \approx \pm\pi$ orange, 40–47s). Dyad 1–3 also dwelled around inphase but for shorter durations (A1, red curve flattening around 12, 22, 32s). The interaction shows tendencies for bistability (inphase and antiphase), as also seen in the histograms of the relative phase (A2), with the orange distribution more pronounced at antiphase than the red. (A3) shows the spatial organizations of phase coordination among agents 1, 3, and 4 at moments corresponding to the time-axis in (A1; for interpretation see B4 below). (B1–4) shows an example of four-person interaction in similar format to the above. Dynamics of ϕ (B1) reveals phase coordination on various time scales, visualized in (B3) where the length of a bar annotates the duration of phase dwell between a pair of participants. Dyad 1–2 (red) showed the longest dwell, Dyad 1–4 (green) a bit shorter, and Dyad 4–3 (blue) the shortest. The coexistence of multiple timescales of coordination gives rise to a constantly evolving spatial organization of the group, shown as a sequence of graphs in (B4) where each node presents a participant and an edge indicates phase dwell (color coding corresponds to B1–3, black edges are dyadic dwells whose dynamics are not shown in B1–2; coordination within the other group, i.e. agents 5, 6, 7, 8, is not shown for reasons of clarity).

<https://doi.org/10.1371/journal.pone.0193843.g001>

coupled agents allows the coexistence of multiple time scales of coordination in a group, as Fig 1A1–1A3 already hinted (orange–long dwell, red–short dwells with more frequent recurrence). Multiple coordinative time scales allow different members of a group to come together at different times, thus allowing the group to visit a variety of spatial patterns at different times. An example of four-person interaction is given in Fig 1B1–1B4 illustrated as three dyadic relative phases (dynamics in B1, distributions in B2). The duration of phase dwells is marked in (B3): red dyad with a long dwell, green dyad a bit shorter, and blue dyad even shorter. Such multiplicity in the time scale of metastable coordination led the four-person group through a variety of spatial patterns from moment to moment (B4) rather than to persist as a static structure (which would be the case if, e.g., phase coordination were absolutely stable). Thus, in the present case of intermediate sized group arrangements, spatiotemporal metastability—coexisting tendencies for integration and segregation—is rather more characteristic of coordination than collective synchronization [50,51].

Dominant patterns of coordination and their relation to diversity

When all phase relations were considered in aggregate, we found that inphase coordination was clearly a dominant phase pattern (central peaks in distributions of relative phase ϕ in Fig 2). Yet this dominance of inphase depended on both local and global diversity. Inphase was more dominant locally within a group (participants paced at the same frequency) than between groups (where diversity was introduced by δf ; Fig 2, A1, probability density for within-group ϕ significantly above chance from 0 to 0.24π , A2, for between-group ϕ significantly above chance from 0.05π to 0.08π , at $\hat{p} < 0.05$, where ‘hat’ denotes Bonferroni correction for multiple comparison throughout the text; see Section G in S1 File for confidence intervals for chance level distribution). Globally, the dominance of inphase in the entire ensemble decreased as diversity increased (B1-3 for $\delta f = 0, 0.3, 0.6$ Hz respectively: B1 significantly above chance from 0 to 0.14π , B2 from 0 to 0.09π , $\hat{p} < 0.05$; B3 n.s.). This suggests that inphase coordination is an important characteristic for the formation and maintenance of coordinative structures regardless of group size, especially when diversity is low. Considering only epochs of strong coordination (dwells), we found a wide range of phase relations, where antiphase, along with inphase, was also a preferable phase relation (for details see Section F in S1 File).

Beyond patterns of phase relations, other types of coordination were observed. One of them is a form of multifrequency coordination that binds behavior at different frequency ratios [14,15,52,53]. We studied which frequency ratios constitute preferred coordination patterns by comparing their probability density to chance levels (computed from randomly permuted

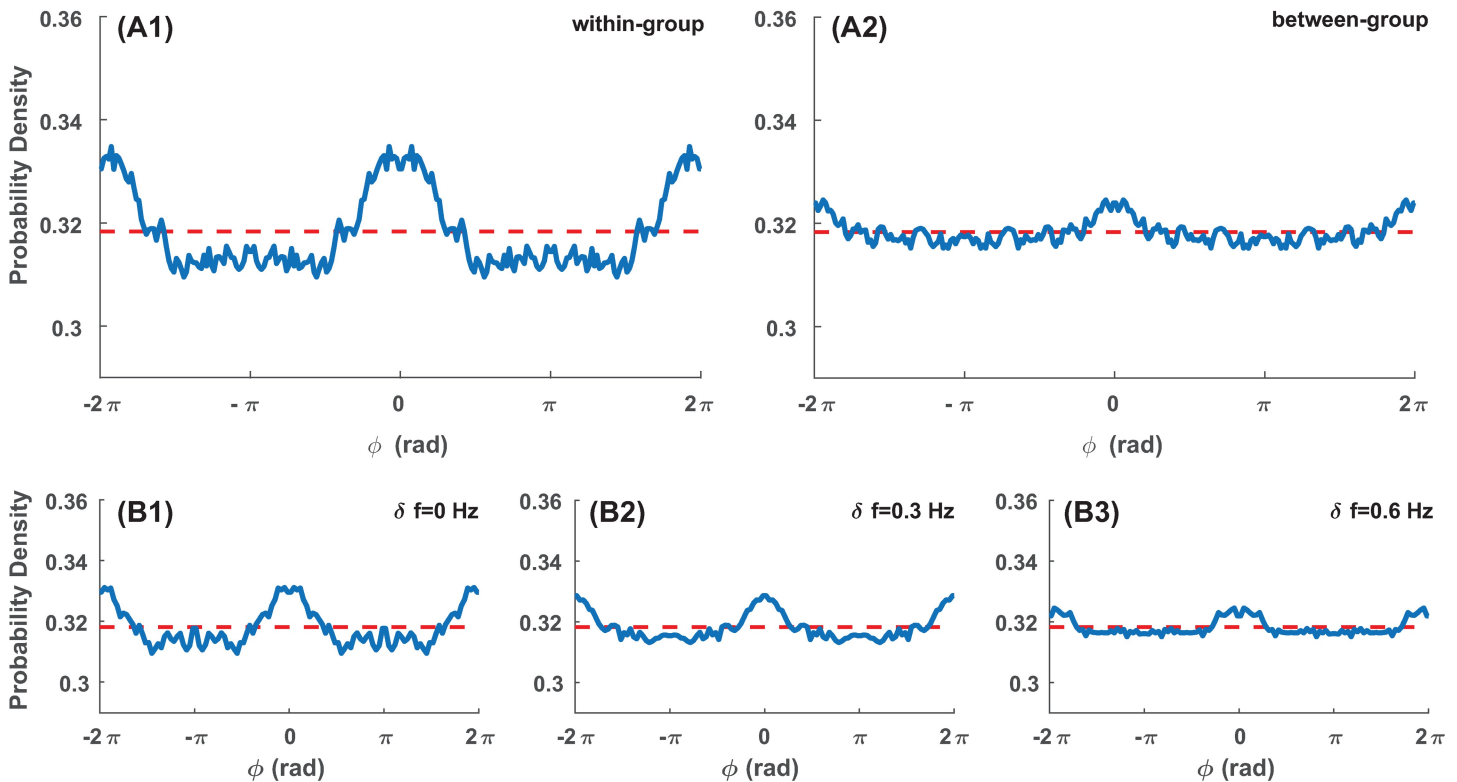


Fig 2. Aggregate distributions of phase relations. Blue solid lines are distributions of relative phases in the experiment (histograms were computed and statistically tested in the interval $[0, \pi]$ then repeated in the interval $[-2\pi, 2\pi]$ for visualization). Red dashed lines correspond to chance level (uniform) distribution. (A1) shows relative phase between members within the same frequency group, (A2) between different groups, (B1-3) for ensembles with diversity level $\delta f = 0, 0.3, 0.6$ Hz respectively. Inphase (central peak) is clearly a dominant pattern throughout, but its dominance diminishes with the diversity parameter displayed in (B1-3). Inphase preference was more pronounced within-group (A1), where participants shared the same initial frequency, than between-group, where frequency diversity was introduced (A2).

<https://doi.org/10.1371/journal.pone.0193843.g002>

taps, see Section D in [S1 File](#) for details). Chance level distributions reflect expected occurrence of different frequency ratios as a result of participants' maintaining metronome frequencies without interacting with each other. Hence, we expected chance level distributions to peak around ratios corresponding to the three diversity conditions, i.e. 1:1 ($\delta f = 0 \text{ Hz}$), 9:11 ($\delta f = 0.3 \text{ Hz}$), and 2:3 ($\delta f = 0.6 \text{ Hz}$). [Fig 3](#) shows the distribution of instantaneous frequency ratios in terms of within-group ([Fig 3A](#)) vs. between-group ([Fig 3B](#)) coordination for different levels of diversity (blue $\delta f = 0 \text{ Hz}$, red $\delta f = 0.3 \text{ Hz}$, yellow $\delta f = 0.6 \text{ Hz}$). A frequency ratio is a preferred coordination pattern if its probability density (solid lines) is above chance level (light-color bands). Within-group participants coordinated primarily at 1:1 ratio ([Fig 3A](#), all $\hat{p} < 0.05$), which is consistent with the high level of phase-locking reported above. For between-group coordination ([Fig 3B](#)), 1:1 was still the preferred ratio when there was no diversity ($\delta f = 0 \text{ Hz}$, $\hat{p} < 0.05$); a higher order ratio near 2:3 was preferred when the diversity was large ($\delta f = 0.6 \text{ Hz}$; $\hat{p} < 0.05$). For intermediate diversity ($\delta f = 0.3 \text{ Hz}$), the between-group frequency coordination was barely above chance at metronome ratio 9:11 (for metronomes at 1.35 Hz and 1.65 Hz), but significantly more concentrated than chance near 1:1 ($\hat{p} < 0.05$). In short, under appropriate diversity conditions, lower order (1:1) and higher order (e.g. ~2:3) frequency coordination can coexist—a basis for complex spatiotemporal coordination. Furthermore, this type of coordination with frequency ratios (one which is less straightforward to detect and less studied) is specific to between-group interactions.

Segregation and integration of groups: Critical diversity

Having studied coordination at the micro level (person to person), we turn now to the macro level of integration and segregation between groups. In order to do so, we first quantified coordination as the level of phase locking between individuals from the same and different initial groups (i.e. within- and between-group coordination respectively). [Fig 4A](#) shows the average results. We found that as initial frequency difference between groups (δf) increased, phase-locking between groups weakened dramatically ([Fig 4A](#), right cluster). Interestingly, phase-locking within groups (no diversity within-group by design) was also weakened by virtue of the difference with the other group ([Fig 4A](#), left cluster, notice orange and yellow bars

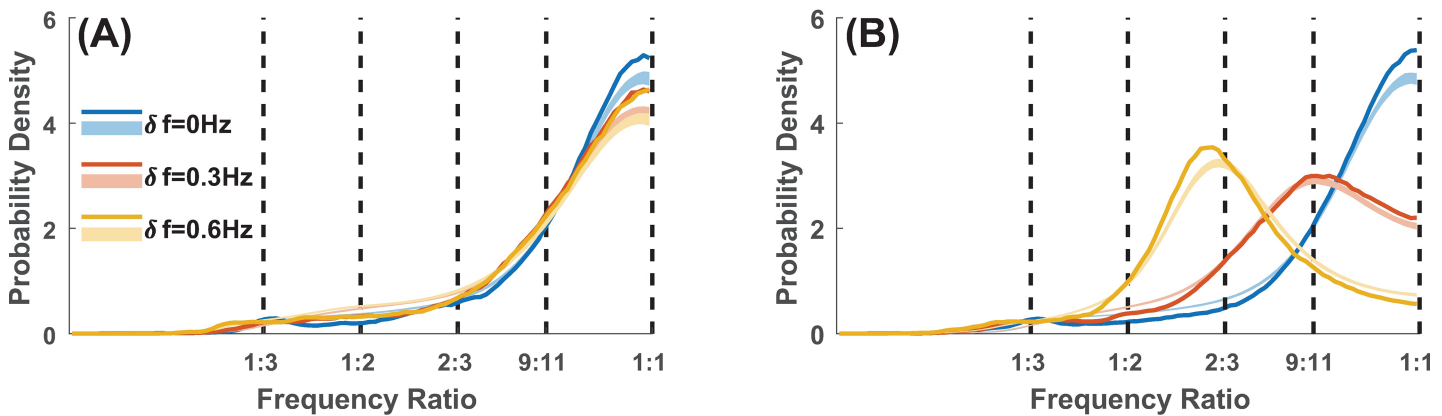


Fig 3. Multifrequency coordination. Ensembles with low diversity were dominated by 1:1 coordination, while ensembles with high diversity also steered towards higher-order ratios. Solid lines show the probability density of frequency relations within- (A) and between-group (B) for the 3 diversity conditions (color coded). Thin shaded areas (with corresponding colors) are confidence intervals for null distributions ($p < 0.0005$ for each of 100 bins, corresponding to $\hat{p} < 0.05$ for an entire distribution using Bonferroni Correction; generated from randomly permuted taps, which represent the expected distribution from non-interacting agents tapping at required frequencies). For within-group relations (A), the peaks at 1:1 are far above chance, indicative of stabilizing phase relations at the same frequency. For between-group relations (B), low to moderate diversity (blue, red, $\delta f = 0, 0.3 \text{ Hz}$) led to above-chance coordination at 1:1; in contrast, for high diversity (yellow, $\delta f = 0.6$, corresponding to metronome ratio 2:3), coordination was below chance at 1:1 but far above chance at a higher order ratio near 2:3.

<https://doi.org/10.1371/journal.pone.0193843.g003>

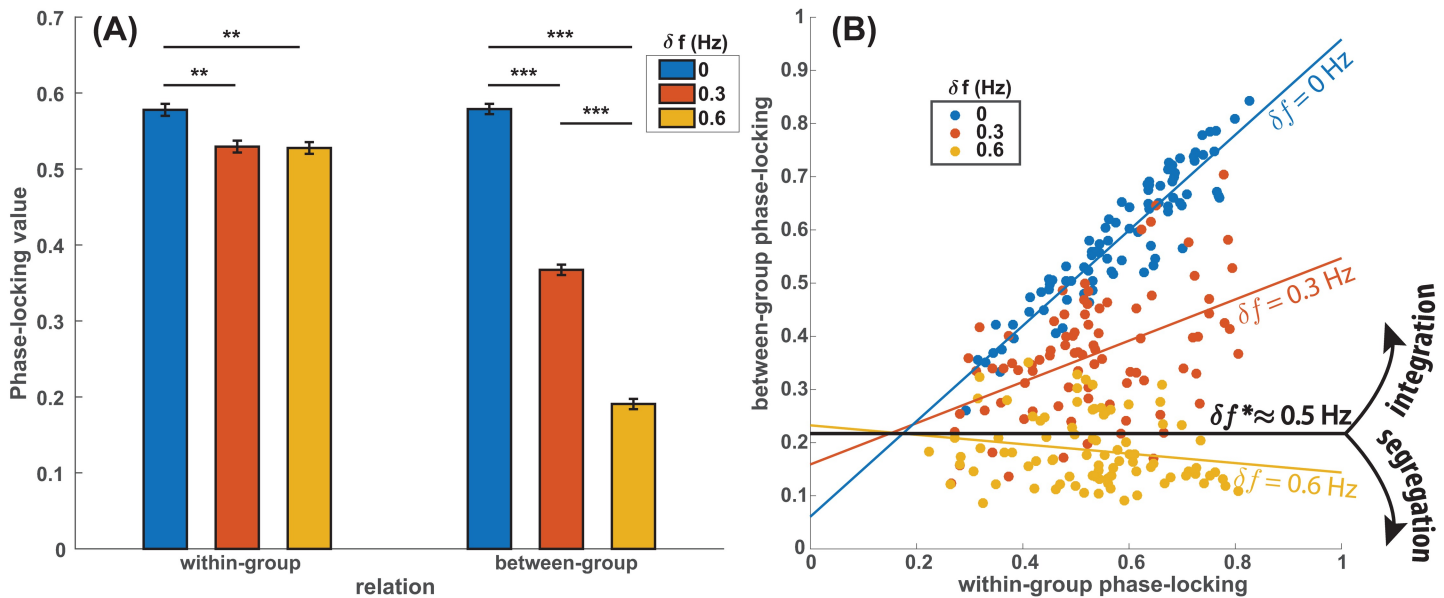


Fig 4. Diversity parametrically controls integration-segregation of groups within ensembles—the emergence of spatial scales. (A) Phase locking between groups decreased monotonically when between-group δf increased (A, right). Within groups however (A, left), where agents' initial frequencies were uniform, phase locking was still affected by the presence of another group of a different frequency (red, yellow bars significantly lower than blue bar), demonstrating that interactions are sensitive to the multiagent context in which they are embedded. (** $p < 0.01$; *** $p < 0.001$; error bars represent standard errors) (B) A scatterplot reveals linear associations between phase locking within- and between-group (each point represents a trial), whose slopes were modulated by the diversity parameter δf (denoted by color, see legend). Linear regressions had positive slope for lower diversity (blue and red colored lines) indicating integration of initial groups into larger coordinative structures, while a negative slope was found for the largest diversity (yellow line), indicating intergroup segregation. A critical parameter of diversity (δf^*) was identified that borders the regimes of integration and segregation (black line).

<https://doi.org/10.1371/journal.pone.0193843.g004>

significantly shorter than blue; MANOVA, interaction effect, $F(2,7246) = 198.2$, $p < 0.001$; see Section L in S1 File for MANOVA main effects analysis). That is, local coordination (e.g. within group) was influenced by the larger context (difference with other groups), as exemplified also in Fig 1A.

Next, we quantified group-level segregation-integration by studying the relation between within-group and between-group coordination. If more within-group coordination leads to more between-group coordination, the groups may be said to become integrated. If more within-group coordination leads to less between-group coordination, the groups may be said to become segregated. In Fig 4B, for the zero intergroup difference ($\delta f = 0$ Hz, blue dots), a large value of within-group phase-locking is paired with a large value of between-group phase-locking, indicating that the initial groups have merged. The same is true, though to a lesser extent, for $\delta f = 0.3$ Hz. For $\delta f = 0.6$ Hz, however, a larger value of within-group phase-locking is associated with a smaller value of between-group phase-locking, suggesting that stronger coordination within the group prevents coordination with members of the other group, or conversely, switching to another group reduces the coordination with one's original group. Quantitatively, for small diversity ($\delta f = 0, 0.3$ Hz), initial groups integrated into one super-group, as seen from the positive slope of regression lines (Fig 4B, blue, red; $\beta_1^{0 \text{ Hz}} = 0.88$, $t(84) = 20.0$, $p < 0.001$; $\beta_1^{0.3 \text{ Hz}} = 0.31$, $t(84) = 3.94$, $p < 0.005$). For larger diversity ($\delta f = 0.6$ Hz), the groups became more segregated (negative slope; Fig 4B, yellow; $\beta_1^{0.6 \text{ Hz}} = -0.14$, $t(85) = -2.83$, $p < 0.01$).

To estimate the critical diversity that marks the boundary between integration and segregation, we regressed the degree of integration $\beta_1^{\delta f}$ against the intergroup difference δf . We found a significant negative linear relation between those variables (linear regression, $\alpha_0 =$

$0.86, t(1) = 20.5, p < 0.05; \alpha_1 = -1.70, t(1) = -15.7, p < 0.05$. By finding when integration vanishes ($\beta_1^{\delta f} = 0$), we identified a critical frequency difference (δf^*) of 0.5 Hz as a boundary between the two different macro-organizations, i.e. a critical value that distinguishes segregation and integration.

Segregation and transitions of spatial order

We now return to real time dynamics to unpack the meaning of macro-level “segregation” in the foregoing statistical conclusion. In an example shown in Fig 5, the ensemble was initially divided into two frequency groups (early on in Fig 5A; faster group of agents 1 to 4, slower group of agents 5 to 8), thanks to the large difference between their metronome frequency ($\delta f = 0.6$ Hz). Soon the ensemble developed into multiple local structures which were coordinated within and segregated between each other (three pairs 3–2, 5–7, 6–8, and two individuals 1, 4; this spatial order can be easily seen in D, first two graphs, 10–25s). The large initial

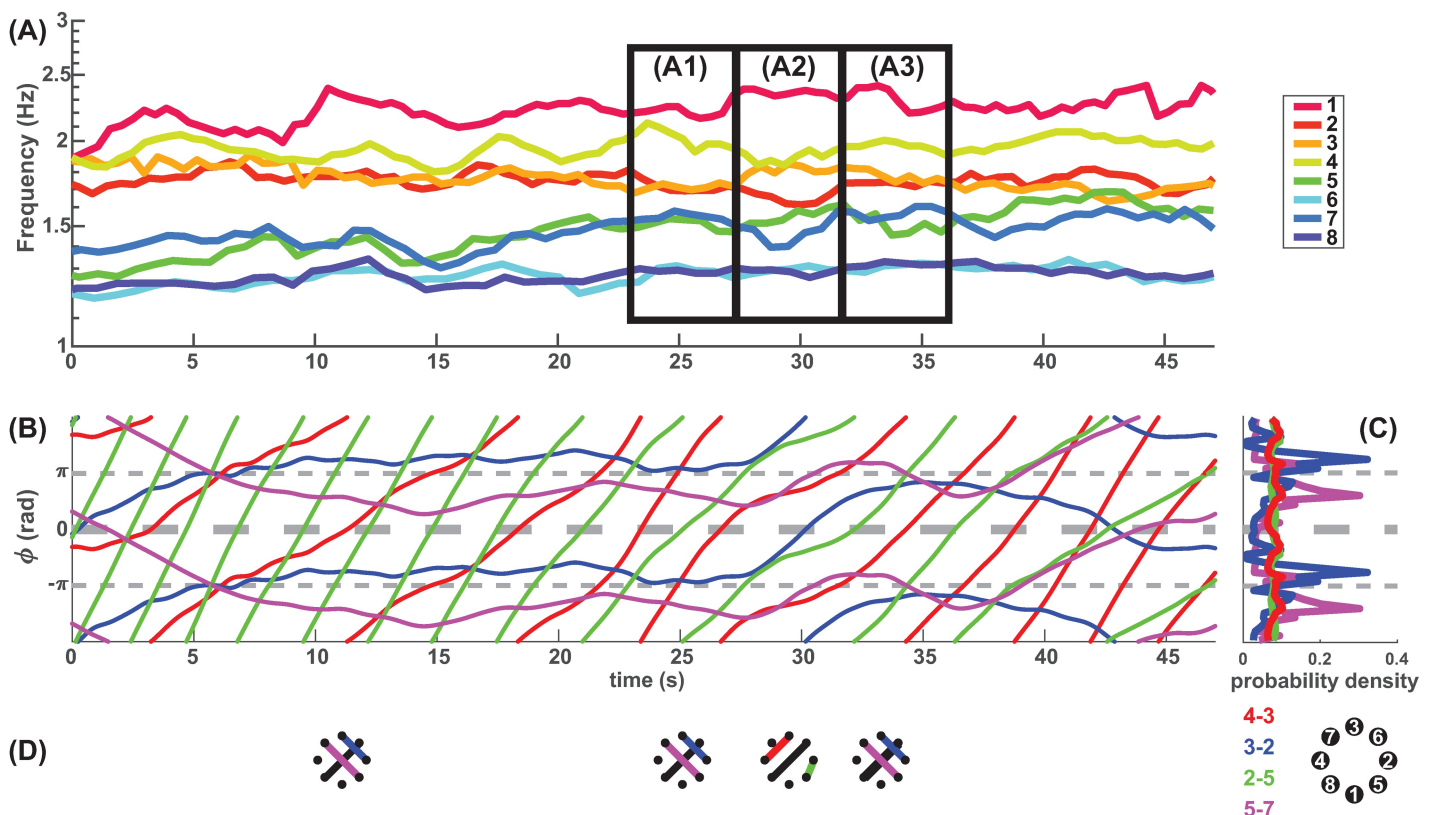


Fig 5. Frequency diversity contributes to spatial organization and reorganization. (A) Instantaneous frequencies of an ensemble of eight interacting agents (smoothed by averaging four consecutive taps). Agents 1 to 4 (warm colors) were paced with the same metronome frequency 1.8 Hz, and similarly agents 5 to 8 (cold colors) were paced at 1.2 Hz, (i.e. $\delta f = 0.6$ Hz), which helped create two initial frequency groups. Soon after the beginning of the interaction (~12s, corresponding to the first graph in D), initial groups divided into five local structures: three pairs (3–2, 5–7, 6–8) and two individuals (agent 1 largely independent, agent 4 oscillating between agent 1 and pair 3–2). The frequency pairing held up to the time of (A1), then a sudden reorganization occurred from (A1) to (A2)—an exchange of partners (3–2 broke up and recoupled into 4–3, 2–5; 7 left alone; corresponding to the 3rd graph in D). The new pairing lasted a few seconds then returned to a similar organization to (A1) at the time of (A3). Phase relations of the pairs involved in the reorganization (A1–3) are illustrated in (B) as time series and in (C) as distributions of four dyadic relative phases. The new organization at A2 lasted exactly the time for pair 3–2 (blue) to break up an antiphase relation (27s) then return to it (33s) after phase wrapping for one cycle. This transition in phase relations corresponds closely to the transitions of frequency grouping. To visualize the spatial consequences of such phase/frequency regrouping, graphs in (D) were used as representations of the coordinative structure. Each node represents a participant at the actual location of the LED representing that participant (up to rotation). Each edge represents the existence of strong phase coordination between two participants at the time (aligned with x-axis in B). The spatial reorganization is apparent from the 2nd and 3rd graph aligned to (A1) and (A2) respectively. Interestingly, the 3rd graph, albeit distinct from the rest, is in fact isomorphic to the other graphs.

<https://doi.org/10.1371/journal.pone.0193843.g005>

diversity allowed the coexistence of multiple segregated groups and enabled the ensemble to form a sustained spatial order by providing sufficient frequency isolation between local structures (in contrast to the low diversity scenario where spatial patterns go through constant reorganization, e.g. Fig 1, Fig H in S1 File). However, a segregated spatial order does not have to be static. To the contrary, there was a sudden transition from one segregated spatial order (A1 and 2nd graph in D) to another, also segregated, spatial order (A2 and 3rd graph in D, a period marked with multiple partner exchanges), then back to the original (A3, and 4th graph in D). This kind of micro-level exchange of members across frequency groups has been observed in 77% of the trials in the segregated condition ($\delta f = 0.6$ Hz). It suggests that segregation is a macro property of ensembles, sustainable despite the coexistence of dynamical exchanges at micro level.

Discussion

Integration and segregation in a diverse group

Rhythmic coordination is ubiquitous in natural systems from the cells of the heart to the neurons of the brain, from fireflies to people [3,39,41,46,54–58]. The convergence of multiple interacting elements to global synchronization has been the focus of experimental and theoretical studies [41–45,59,60]. Behavioral synchronization is known to facilitate social communication and the development of social affection or bonding [61–65], and is important to understanding social coordination dynamics [66,67]. Nevertheless, within a community, people coordinate in multiple social groups at various spatiotemporal scales—a complex organization that is far from uniform synchronization [68–70]. In fact, the components of living systems often compartmentalize into distinct communities or modules, highlighted by dense interactions within communities and loose interactions between communities [71,72]. This form of organization, embracing both integration and segregation among its elements, can lead to greater persistence and robustness of the system [73–76], and influence structural and functional complexity depending on the scale of integration [77–79]. Investigation of the conditions leading to the formation, change, and dissolution of segregated structures is a necessary step to understanding and controlling complex systems.

We demonstrated experimentally how coexisting groups integrated and segregated in an ensemble of eight interacting people. Each half of the ensemble was predisposed to move at a distinct frequency prior to social interaction, thereby creating two initial frequency groups with a controllable parameter of diversity between them (δf). People engaged in more phase coordination with those who were predisposed to move at the same frequency than with those who performed at a different frequency (Fig 4A; Fig K in S1 File left). This is a form of “homophily”—people prefer interacting with those who are similar to themselves than with those who are different [80]—known to contribute to segregation in diverse communities [81–84]. Indeed, the integrating force of sameness is complemented by the segregating force of difference [85].

To what extent do quantitative changes in intergroup diversity induce a qualitative change in intergroup relationships? We have shown that low-to-moderate diversity led to integration of the groups ($\delta f = 0, 0.3$ Hz; Fig 1B): more coordination within-group was associated with more coordination between-group. High intergroup diversity led to segregation ($\delta f = 0.6$ Hz; Fig 1B): more coordination within-group was associated with less coordination between-group. Parametrically varying diversity made it possible to estimate the critical value of diversity (δf^*): exceeding this critical value led to segregation; remaining below the critical value led to integration. Identifying the critical values of a dynamical system empirically proves to be a valuable step in many situations, not only to provide essential information on the organizing

principles and potential behaviors of the system, but also to serve as key phenomena to be reproduced in theoretical models [86,87].

A complex system consists of interactions at multiple spatial scales, where activities at one scale are connected with those of another scale [88,89]. How the macro environment constrains micro activities was illuminated by comparing dyadic interactions embedded in a group with expected behavior of dyads in isolation. If dyads (micro) were not influenced by the larger environmental context (macro), the same amount of coordination would be observed within groups at all three levels of intergroup diversity. The data say otherwise: phase locking within a group was in fact weakened by intergroup diversity (Fig 4A, left). This shows that when a system has multiple components, dyadic interactions may not be fully understood without taking into account the larger environment or context they are embedded in [4,90,91].

The patterns of coordination

To further understand the micro dynamics of social interaction, we identified the specific phase patterns people adopted. Overall, we found that inphase was visited significantly more often than other phase relation, yet its prominence diminished with increasing diversity (Fig 2). That is, diversity induced a dispersion of phase patterns. Absolute synchronization between components' behavior is not always desirable: excessive synchrony may induce pathological collective dynamics [92] or impede complex functions [79,93]. Diversity may come to the rescue. Besides inphase, a preference of antiphase over various other phase relations also stood out in episodes of strong interactions (Fig C in S1 File). The present results resonate with existing studies of human rhythmic coordination [3,30]. When coupling was sufficiently strong, the tendency for two oscillatory components to coordinate inphase or antiphase was found across scales, particularly when the components have similar frequency predispositions [94]. When coupling was sufficiently weak, however, the antiphase pattern was more vulnerable to natural frequency differences [32,47]. Both diversity in frequency predispositions [11] and multiagent environment [35,37,95–97] help engender a variety of phase relations that are neither inphase nor antiphase. The agreement between the statistical properties of the interactive behaviors in an ensemble of eight persons and the dynamic properties of dyadic coordination suggests that dyads remain the most stable unit of spontaneous coordination. Yet how can group coordination be achieved with primarily dyadic interactions? This led us to explore the dynamics of phase relations.

Phase relations do not have to be static, as social coordination often evolves on multiple time scales [68,69,98]. Over the course of interaction, we found that most phase relations only lasted a short period of time (4–5s, Fig B in S1 File). Two partners dwell in a phase relation for a few seconds before a “breakup” or “escape” from that relation, and then re-engage the next time they come across a favorable phase relation (e.g. Fig 1). The recurrent relation embodied by a series of dwells and escapes is characteristic of metastable coordination dynamics [50,94,99]. Theoretically and empirically, metastability occurs in weakly coupled dynamical systems when there is sufficient difference in the components' frequency predispositions. The combination of symmetry breaking and weak coupling eliminates perfectly stable phase relations which are replaced by intermittent or recurrent phasing. In the present study, quantitative analysis confirms that metastability prevails in all conditions of interaction (Fig J in S1 File). Notice that the sequence of dwells and escapes of phase relations also manifests as oscillations in movement frequency (e.g. Fig G in S1 File). In contrast with stable coordination in which components eventually converge to the same frequency, metastability allows components to visit a range of frequencies while still maintaining “social bonds” via intermittent dwells. When multiple metastable relations coexist in the same group, it becomes possible for a

person's transient escape from an existing relation to be at the same time a dwell in a new relation. This chimeric feature (c.f. [51]) allows members of a community to participate in multiple segregated substructures (e.g. a reading club, and a hiking team) while maintaining both the separability of those substructures and communication between them. Such continuous change of membership helps large communities to persist [100] and increase global level of cooperation [101]. Spatiotemporal metastability in multiple-component systems suits both the intuition of daily social interaction, as well as the dynamic patterns observed in large scale social networks [68].

Phase-locking constitutes a rather strong form of coordination. Such coordination comes at a cost in both time and energy if the partners possess different frequency predispositions: the chasm of frequency difference, jointly or unilaterally, must somehow be crossed. In the present experiment, not all forms of coordination required such costly crossovers. As diversity increased, people from different groups were found to adopt particular frequency relations (or ratios) of higher order (e.g. near 2:3, Fig 3B, yellow) as opposed to converging to a single frequency (1:1). Frequency relations appear in the more familiar context of music as polyrhythms. Theoretical and experimental studies have shown the viability of different frequency ratios: higher order ratios (e.g. 2:5, 3:5) are more difficult to maintain (less stable) than lower order ratios (e.g. 1:3, 2:3) in accordance with so-called Arnold tongue and Farey tree principles [15,53,102,103]. Such frequency relations enable segregated groups to maintain communication between each other, without sacrificing within-group cohesion, thus allowing complex coordinative structures to form. Such cross-frequency communication may serve to integrate local activities over long distance and time scales in complex systems, including the brain [89,104,105].

Conclusions

Our goal was to elucidate the coordination dynamics of ensembles of eight people, where the ensemble is small enough for systematic manipulation in the laboratory, but not too small as to prevent the unfolding of complex social dynamics (i.e., simple, but no simpler). At the macro level, we studied the integration and segregation of groups and how it affects, at the micro level, dyadic interactions embedded within. A novel finding was that the domains of integration and segregation between groups are demarcated by a critical level of intergroup diversity. Diversity across groups also affected the strength and forms of dyadic coordination within groups. In particular, a metastable form of phase coordination was revealed in which phase relations were intermittent rather than stable, thereby allowing people to switch flexibly between partners as a means of maintaining both diversity and unity. When groups were segregated and phase coordination became difficult, social coordination also took the form of cross-frequency coupling. The present work provides a multiscale portrait of the coordination dynamics among multiple agents, and thereby offers quantitative details and reality checks for modelling social dynamics. The analytical methods used here can be extended to study segregation and integration in larger systems, where an abundance of scales of interaction is likely to further unveil the complexity and stability of large scale networks or coordinative structures.

Materials and methods

Participants

120 participants (76 female, age 24 ± 8 yrs.) participated in the experiment, making up 15 independent ensembles of eight. All participants were right-handed except 4, who were all able to complete the tasks without difficulty. The protocol was approved by Florida Atlantic

University Institutional Review Board and in agreement with the Declaration of Helsinki. Written informed consent was obtained from all participants prior to the experiment.

Experimental setup

For each ensemble of eight, participants were randomly seated in booths around an octagonal table. They did not have direct visual contact with each other. Each participant was equipped with a touchpad (green rectangle in Fig 6) and an array of eight light-emitting photodiodes (LEDs; yellow in Fig 6). Each tap of a participant was broadcast to all participants (including self) in real time as a single flash of an assigned LED (hand contacts touchpad, light on; hand leaves touchpad, light off). The tap~flash signals were converted and transmitted through a signal processing pipeline consisting of a PC flanked by two microcontrollers (MCs; one for input, one for output; communicates with the PC through serial port at 57600 bps). The input MC samples movement data from the touchpads at 250 Hz (1 = touch, 0 = leave) and sends data to the PC. Dedicated software (written in C++) runs on the PC, which receives tapping

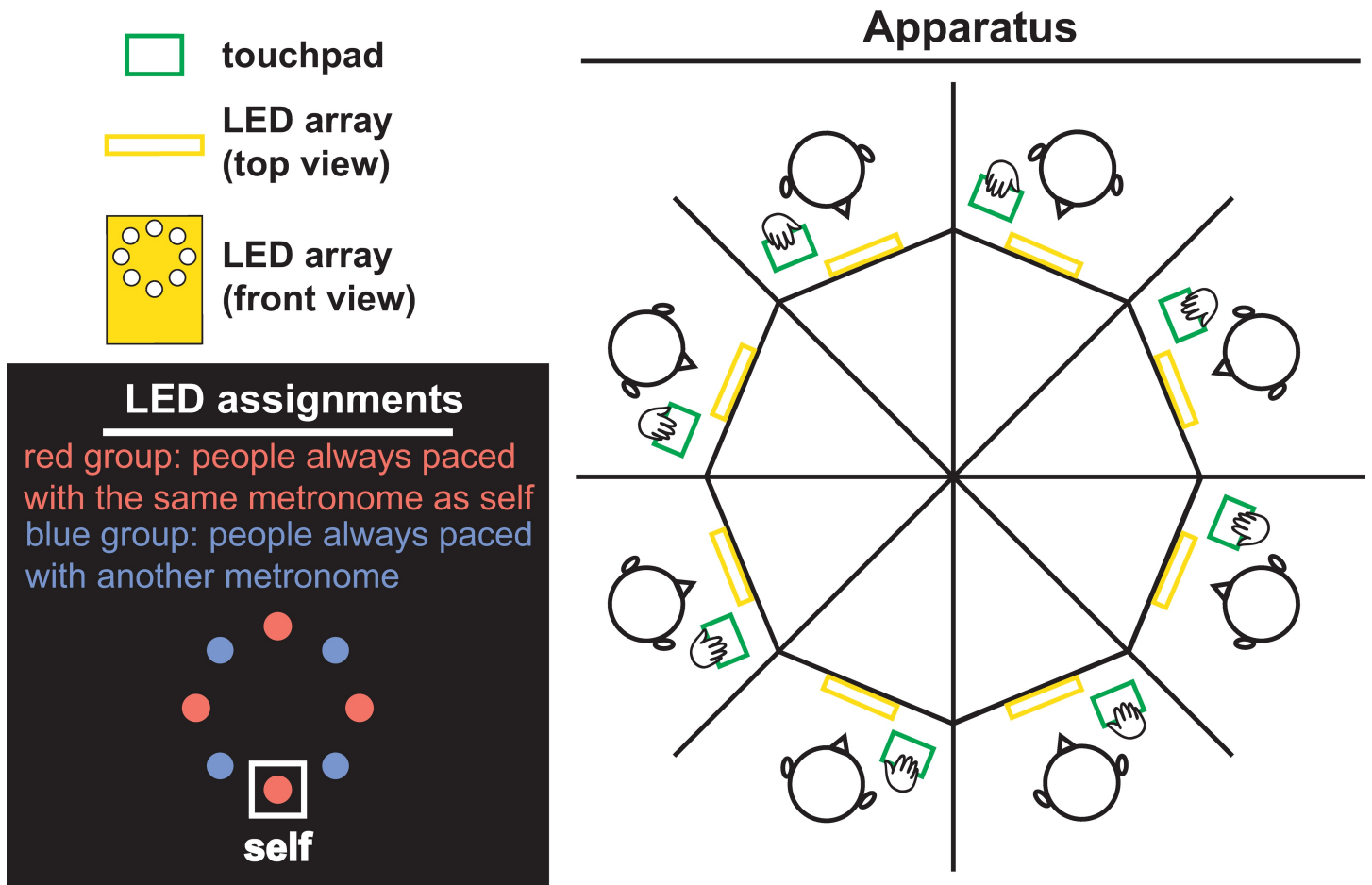


Fig 6. Experimental setup. Eight participants are seated around an octagonal table; they do not have direct vision of each other. Rather, they are exposed to each other's tapping behavior through touchpads (record tapping; green) and arrays of LEDs (display self and others' taps as flashes; yellow). On each LED array, there is a one-to-one correspondence between LEDs and participants. (black box) The mapping was rotated for each array so that a participant always saw self-behavior at the lowest LED (white box). All LEDs labeled red represent people who were paced by metronomes of the same frequency as for self. LEDs labelled blue represent people paced to metronomes at another frequency (actual LEDs were all in the same color). By such metronome assignment, participants of the same ensemble were split into two initial frequency groups. By manipulating the metronome difference between the two groups, we created different levels of diversity, thereby inducing integration~segregation at different spatial scales.

<https://doi.org/10.1371/journal.pone.0193843.g006>

data from the input MC, and controls the spatial configuration of LEDs and the network connectivity among participants. The spatial configuration map assigns each LED on each array to represent a particular participant. The spatial configuration map was randomized across different ensembles of eight, but fixed for each ensemble throughout an experimental session. In this particular experiment, the network connectivity map determines whether a particular participant can see (1) only self-produced flashes; (2) self-produced flashes and a metronome (computer generated flashes, see **Procedures**); or (3) self- and other-produced flashes. After the spatial and network mapping are completed, the PC sends 64 bit data to 8 LED arrays via the output MC, synchronized to each sample from the input MC (tap-to-flash latency 2.5–4.5ms, less than 1% of the shortest period of metronomes).

Procedures

Each trial of the experiment lasted 68s and consisted of three stages. In *Stage 1* (5s), participants tapped rhythmically at their own comfortable frequency, only seeing self-produced flashes ([Fig 6](#), black inset “self”). In *Stage 2* (10s), all the non-self LEDs started to flash in synchrony at a preassigned frequency, basically a metronome (initial phase randomized). Participants were instructed to match their own tapping frequency to the metronome frequency, and remain tapping at that frequency throughout the rest of the trial even after the metronome disappeared. Following a 3s transient, subjects were exposed to each other’s rhythmic behavior (*Stage 3*, 50s), each LED flashed corresponding to a particular participant’s taps.

We manipulated intergroup behavior by assigning metronomes of different frequencies to different participants. In order to emphasize frequency diversity, spatial symmetry was imposed as follows: from each participant’s perspective, persons presented at the north, west, and east of the center of the LED array were always paced with the same metronome as self (south to center), whilst the others were paced with another metronome. Thus, metronome assignment was designed to split eight people into two initial frequency groups (red group and blue group in [Fig 6](#), black inset). Diversity thus appears across groups not within groups. Specifically, for each trial, group metronomes were assigned following one of the three conditions: (1) 1.5 Hz vs. 1.5 Hz, (2) 1.65 Hz vs. 1.35 Hz, and (3) 1.8 Hz vs. 1.2 Hz. With the same mean frequency (1.5Hz), the three conditions correspond to three levels of between-group metronome difference (δf) which we term a diversity parameter: $\delta f = 0$ Hz, $\delta f = 0.3$ Hz, $\delta f = 0.6$ Hz.

Each ensemble of eight participants completed 24 trials in random order, including 6 trials in which participants were only connected to people within their own group (results not reported in this paper) and 18 trials in which every participant was connected to every other participant. In the present paper, we consider the effect of different levels of between-group difference on fully connected ensembles of eight people.

Statistical analyses

Distributions of relative phase (ϕ) and frequency ratio (FR) were compared to chance level using permutation tests. Ten thousand randomly permuted time series were used for constructing the confidence intervals of chance level distributions. The significance level was chosen to be $\hat{\alpha} = 0.05$ (with Bonferroni correction). Computational details are shown in Section A and Section D in [S1 File](#).

To compare the level of phase-locking in different conditions, two-way ANOVA was used (2×3 for relation $\times \delta f$) with Type III Sums of Squares; Tukey Honest Significant Difference tests were used for post hoc comparisons (see Section B in [S1 File](#) for details).

To measure the level of integration between groups, we regressed the level of within-group phase locking against between group phase-locking separately for 3 diversity levels. The slopes

of the regression lines ($\beta_1^{\delta f}$) reflect the level of integration (positive slope = integration, negative slope = segregation). The critical level of diversity (δf^*), corresponding to zero-slope ($\beta_1 = 0$), was found through linear interpolation (see Section C in [S1 File](#) for details).

Supporting information

S1 File. Supporting information. Re: “Critical diversity: divided or united states of social coordination” by Zhang et al.
(PDF)

Acknowledgments

This work was supported by the National Institute of Mental Health (MH080838), the Chaire d’Excellence Pierre de Fermat, and the Davimos Family Endowment for Excellence in Science. The paper is dedicated to Dr. Thomas C. Schelling, who passed away on December 13, 2016 and is best known to complex system scientists for his seminal paper “Dynamic models of segregation” (1971, *The Journal of Mathematical Sociology*). We thank Dr. Roxana Stefanescu for assisting in data collection.

Author Contributions

Conceptualization: Mengsen Zhang, J. A. Scott Kelso, Emmanuelle Tognoli.

Data curation: Mengsen Zhang.

Formal analysis: Mengsen Zhang.

Funding acquisition: J. A. Scott Kelso, Emmanuelle Tognoli.

Investigation: Mengsen Zhang.

Methodology: Mengsen Zhang, Emmanuelle Tognoli.

Project administration: Emmanuelle Tognoli.

Resources: J. A. Scott Kelso, Emmanuelle Tognoli.

Software: Mengsen Zhang.

Supervision: J. A. Scott Kelso, Emmanuelle Tognoli.

Validation: Mengsen Zhang, Emmanuelle Tognoli.

Visualization: Mengsen Zhang.

Writing – original draft: Mengsen Zhang.

Writing – review & editing: Mengsen Zhang, J. A. Scott Kelso, Emmanuelle Tognoli.

References

1. Haken H. Synergetics: Introduction and Advanced Topics. Berlin, Heidelberg: Springer Berlin Heidelberg; 2004. <https://doi.org/10.1007/978-3-662-10184-1>
2. Camazine S, Deneubourg J-L, Franks NR, Sneyd J, Theraulaz G, Bonabeau E. Self-Organization in Biological Systems. Princeton University Press; 2003.
3. Kelso JAS. Dynamic Patterns: The Self-Organization of Brain and Behavior. Cambridge, Massachusetts: The MIT Press; 1995.
4. Miller JH, Page SE. Complex Adaptive Systems: an Introduction to Computational Models of Social Life. Princeton university press; 2009.

5. Brown FA. Living clocks: the clocks are accounted for as “open systems” depending upon subtle geo-physical rhythms. *Science*. 1959; 130: 1535–1544. <https://doi.org/10.1126/science.130.3388.1535> PMID: 13804924
6. Wunderlich FM. Symphonies of urban places: urban rhythms as traces of time in space a study of “urban rhythms.” *Place Locat Stud Environ Aesthet Semiot VI*. 2008; 91–111.
7. Glass L. Synchronization and rhythmic processes in physiology. *Nature*. 2001; 410: 277–284. <https://doi.org/10.1038/35065745> PMID: 11258383
8. Buzsáki G. Rhythms of the Brain. Oxford University Press; 2006. <https://doi.org/10.1093/acprof:oso/9780195301069.001.0001>
9. Blasius B, Huppert A, Stone L. Complex dynamics and phase synchronization in spatially extended ecological systems. *Nature*. 1999; 399: 354–9. <https://doi.org/10.1038/20676> PMID: 10360572
10. Repp BH. Sensorimotor synchronization: a review of the tapping literature. *Psychon Bull Rev*. 2005; 12: 969–992. <https://doi.org/10.3758/BF03206433> PMID: 16615317
11. Kelso JAS, Del Colle JD, Schöner G. Action-perception as a pattern formation process. *Attention and performance 13: Motor representation and control*. Hillsdale, NJ, US: Lawrence Erlbaum Associates, Inc; 1990. pp. 139–169.
12. Kelso JAS. Phase transitions and critical behaviour in human bimanual coordination. *Am J Physiol Regul Integr Comp Physiol*. 1984; 246: R1000–1004.
13. Schöner G, Kelso JAS. Dynamic pattern generation in behavioral and neural systems. *Science*. 1988; 239: 1513–1520. <https://doi.org/10.1126/science.3281253> PMID: 3281253
14. Assisi CG, Jirsa VK, Kelso JAS. Dynamics of multifrequency coordination using parametric driving: theory and experiment. *Biol Cybern*. 2005; 93: 6–21. <https://doi.org/10.1007/s00422-005-0558-y> PMID: 15926066
15. Peper CE, Beek PJ, van Wieringen PCW. Multifrequency coordination in bimanual tapping: Asymmetrical coupling and signs of supercriticality. *J Exp Psychol Hum Percept Perform*. 1995; 21: 1117–1138. <https://doi.org/10.1037/0096-1523.21.5.1117>
16. Oullier O, de Guzman GC, Jantzen KJ, Lagarde J, Kelso JAS. Social coordination dynamics: measuring human bonding. *Soc Neurosci*. 2008; 3: 178–192. <https://doi.org/10.1080/17470910701563392> PMID: 18552971
17. Richardson MJ, Marsh KL, Isenhower RW, Goodman JRL, Schmidt RC. Rocking together: dynamics of intentional and unintentional interpersonal coordination. *Hum Mov Sci*. 2007; 26: 867–891. <https://doi.org/10.1016/j.humov.2007.07.002> PMID: 17765345
18. Tognoli E, Lagarde J, de Guzman GC, Kelso JAS. The phi complex as a neuromarker of human social coordination. *Proc Natl Acad Sci*. 2007; 104: 8190–8195. <https://doi.org/10.1073/pnas.0611453104> PMID: 17470821
19. Dumas G, Nadel J, Soussignan R, Martinerie J, Garnero L. Inter-brain synchronization during social interaction. Lauweryens J, editor. *PLoS One*. 2010; 5: e12166. <https://doi.org/10.1371/journal.pone.0012166> PMID: 20808907
20. Noy L, Dekel E, Alon U. The mirror game as a paradigm for studying the dynamics of two people improvising motion together. *Proc Natl Acad Sci*. 2011; 108: 20947–20952. <https://doi.org/10.1073/pnas.1108155108> PMID: 22160696
21. Hasson U, Ghazanfar AA, Galantucci B, Garrod S, Keysers C. Brain-to-brain coupling: a mechanism for creating and sharing a social world. *Trends Cogn Sci*. 2012; 16: 114–121. <https://doi.org/10.1016/j.tics.2011.12.007> PMID: 22221820
22. Schmidt RC, Carello C, Turvey MT. Phase transitions and critical fluctuations in the visual coordination of rhythmical movements between people. *J Exp Psychol Hum Percept Perform*. 1990; 16: 227–247. <https://doi.org/10.1037/0096-1523.16.2.227> PMID: 2142196
23. Varela F, Lachaux JP, Rodriguez E, Martinerie J. The brainweb: phase synchronization and large-scale integration. *Nat Rev Neurosci*. 2001; 2: 229–239. <https://doi.org/10.1038/35067550> PMID: 11283746
24. Tognoli E, Kelso JAS. Brain coordination dynamics: true and false faces of phase synchrony and metastability. *Prog Neurobiol*. 2009; 87: 31–40. <https://doi.org/10.1016/j.pneurobio.2008.09.014> PMID: 18938209
25. Kelso JAS, de Guzman GC, Reveley C, Tognoli E. Virtual Partner Interaction (VPI): exploring novel behaviors via coordination dynamics. Sporns O, editor. *PLoS One*. 2009; 4: e5749. <https://doi.org/10.1371/journal.pone.0005749> PMID: 19492044
26. Dumas G, de Guzman GC, Tognoli E, Kelso JAS. The human dynamic clamp as a paradigm for social interaction. *Proc Natl Acad Sci*. 2014; 111: E3726–E3734. <https://doi.org/10.1073/pnas.1407486111> PMID: 25114256

27. Kostrubiec V, Dumas G, Zanone P-G, Kelso JAS. The Virtual Teacher (VT) paradigm: learning new patterns of interpersonal coordination using the Human Dynamic Clamp. Marinazzo D, editor. PLoS One. 2015; 10: e0142029. <https://doi.org/10.1371/journal.pone.0142029> PMID: 26569608
28. Lagarde J, Peham C, Licka T, Kelso JAS. Coordination dynamics of the horse-rider system. J Mot Behav. 2005; 37: 418–424. <https://doi.org/10.3200/JMBR.37.6.418-424> PMID: 16280312
29. Pfau T, Spence A, Starke S, Ferrari M, Wilson A. Modern riding style improves horse racing times. Science. 2009; 325: 289–289. <https://doi.org/10.1126/science.1174605> PMID: 19608909
30. Haken H, Kelso JAS, Bunz H. A theoretical model of phase transitions in human hand movements. Biol Cybern. 1985; 51: 347–356. <https://doi.org/10.1007/BF00336922> PMID: 3978150
31. Schöner G, Kelso JAS. A dynamic pattern theory of behavioral change. J Theor Biol. 1988; 135: 501–524. [https://doi.org/10.1016/S0022-5193\(88\)80273-X](https://doi.org/10.1016/S0022-5193(88)80273-X)
32. Fuchs A, Jirsa VK, Haken H, Kelso JAS. Extending the HKB model of coordinated movement to oscillators with different eigenfrequencies. Biol Cybern. 1996; 74: 21–30. <https://doi.org/10.1007/BF00199134> PMID: 8573650
33. Schöner G, Haken H, Kelso JAS. A stochastic theory of phase transitions in human hand movement. Biol Cybern. 1986; 53: 247–257. <https://doi.org/10.1007/BF00336995> PMID: 3955100
34. Schöner G, Jiang WY, Kelso JAS. A synergistic theory of quadrupedal gaits and gait transitions. J Theor Biol. 1990; 142: 359–391. PMID: 2338828
35. Collins JJ, Stewart I. Coupled nonlinear oscillators and the symmetries of animal gaits. J Nonlinear Sci. 1993; 3: 349–392. <https://doi.org/10.1007/BF02429870>
36. Jeka JJ, Kelso JAS. Manipulating symmetry in the coordination dynamics of human movement. J Exp Psychol Hum Percept Perform. 1995; 21: 360–374. PMID: 7714477
37. Golubitsky M, Stewart I, Buono P-LL, Collins JJ. Symmetry in locomotor central pattern generators and animal gaits. Nature. 1999; 401: 693–695. <https://doi.org/10.1038/44416> PMID: 10537106
38. Kelso JAS, Jeka JJ. Symmetry breaking dynamics of human multilimb coordination. J Exp Psychol Hum Percept Perform. 1992; 18: 645–668. <https://doi.org/10.1037/0096-1523.18.3.645> PMID: 1500867
39. Buck J, Buck E. Synchronous fireflies. Sci Am. 1976; 234: 74–85. <https://doi.org/10.1038/scientificamerican0576-74> PMID: 1273569
40. Edelman GM, Tononi GS. Reentry and the dynamic core: neural correlates of conscious experience. In: Metzinger T, editor. Neural Correlates of Consciousness. MIT Press; 2000.
41. Néda Z, Ravasz E, Brechet Y, Vicsek T, Barabási A-L. The sound of many hands clapping. Nature. 2000; 403: 849–850. <https://doi.org/10.1038/35002660> PMID: 10706271
42. Strogatz SH. From Kuramoto to Crawford: exploring the onset of synchronization in populations of coupled oscillators. Phys D Nonlinear Phenom. 2000; 143: 1–20. [https://doi.org/10.1016/S0167-2789\(00\)00094-4](https://doi.org/10.1016/S0167-2789(00)00094-4)
43. Kuramoto Y. Chemical Oscillations, Waves and Turbulence. [Internet]. Berlin: Springer; 1983. <https://doi.org/10.1007/978-3-642-12601-7>
44. Néda Z, Ravasz E, Vicsek T, Brechet Y, Barabási A-L. Physics of the rhythmic applause. Phys Rev E —Stat Physics, Plasmas, Fluids, Relat Interdiscip Top. 2000; 61: 6987–6992. <https://doi.org/10.1103/PhysRevE.61.6987>
45. Mirollo RE, Strogatz SH. Synchronization of pulse-coupled biological oscillators. SIAM J Appl Math. 1990; 50: 1645–1662.
46. Richardson MJ, Garcia RL, Frank TD, Gergor M, Marsh KL. Measuring group synchrony: a cluster-phase method for analyzing multivariate movement time-series. Front Physiol. 2012; 3: 1–10. <https://doi.org/10.3389/fphys.2012.00001> PMID: 22275902
47. Fuchs A. Nonlinear Dynamics in Complex Systems. Berlin, Heidelberg: Springer Berlin Heidelberg; 2013. <https://doi.org/10.1007/978-3-642-33552-5>
48. Kelso JAS. Multistability and metastability: understanding dynamic coordination in the brain. Philos Trans R Soc B Biol Sci. 2012; 367: 906–918. <https://doi.org/10.1098/rstb.2011.0351> PMID: 22371613
49. Von Holst E. On the nature of order in the central nervous system. The Collected Papers of Erich von Holst Vol 1, The Behavioral Physiology of Animal and Man. Coral Gables, FL.: University of Miami Press; 1973. pp. 3–32.
50. Tognoli E, Kelso JAS. The metastable brain. Neuron. Elsevier Inc.; 2014; 81: 35–48. <https://doi.org/10.1016/j.neuron.2013.12.022> PMID: 24411730
51. Kelso JAS. The dynamic brain in action: coordinative structures, criticality, and coordination dynamics. In: Plenz D, Niebur E, editors. Criticality in Neural Systems. 2014. pp. 67–104. <https://doi.org/10.1002/9783527651009.ch4>

52. de Guzman GC, Kelso JAS. Multifrequency behavioral patterns and the phase attractive circle map. *Biol Cybern.* 1991; 64: 485–495. <https://doi.org/10.1007/BF00202613> PMID: 1863660
53. Kelso JAS, de Guzman GC. Order in time: how the cooperation between the hands informs the design of the brain. In: Haken H, editor. *Neural and Synergetic Computers*. Berlin, Heidelberg: Springer Berlin Heidelberg; 1988. pp. 180–196. https://doi.org/10.1007/978-3-642-74119-7_13
54. Strogatz SH, Goldenfeld N. Sync: The emerging science of spontaneous order. *Phys Today.* 2004; 57: 59–60. <https://doi.org/10.1063/1.1784276>
55. Buck J. Synchronous rhythmic flashing of fireflies. II. *Q Rev Biol.* 1988; 63: 265–289. <https://doi.org/10.1086/415929> PMID: 3059390
56. Strogatz SH, Stewart I. Coupled oscillators and biological synchronization. *Sci Am.* 1993; 269: 102–109. <https://doi.org/10.1038/scientificamerican1293-102> PMID: 8266056
57. Winfree AT. *The Geometry of Biological Time* [Internet]. Springer. New York, NY: Springer New York; 2001. <https://doi.org/10.1007/978-1-4757-3484-3>
58. Buzsáki G. Theta rhythm of navigation: link between path integration and landmark navigation, episodic and semantic memory. *Hippocampus.* 2005; 15: 827–840. <https://doi.org/10.1002/hipo.20113> PMID: 16149082
59. Alderisio F, Bardy BG, di Bernardo M. Entrainment and synchronization in networks of Rayleigh–van der Pol oscillators with diffusive and Haken–Kelso–Bunz couplings. *Biol Cybern.* Springer Berlin Heidelberg; 2016; 110: 151–169. <https://doi.org/10.1007/s00422-016-0685-7> PMID: 27108135
60. Nishikawa T, Motter AE. Symmetric states requiring system asymmetry. *Phys Rev Lett.* 2016; 117: 1–5. <https://doi.org/10.1103/PhysRevLett.117.114101>
61. Valdesolo P, DeSteno D. Synchrony and the social tuning of compassion. *Emotion.* 2011; 11: 262–266. <https://doi.org/10.1037/a0021302> PMID: 21500895
62. Hove MJ, Risen JL. It's all in the timing: interpersonal synchrony increases affiliation. *Soc Cogn.* 2009; 27: 949–960. <https://doi.org/10.1521/soco.2009.27.6.949>
63. Zhang M, Dumas G, Kelso JAS, Tognoli E. Enhanced emotional responses during social coordination with a virtual partner. *Int J Psychophysiol.* 2016; 104: 33–43. <https://doi.org/10.1016/j.ijpsycho.2016.04.001> PMID: 27094374
64. Fogel A, Nwokah E, Dedo JY, Messinger D. Social process theory of emotion: A dynamic systems approach. *Soc Dev.* 1992; 1: 122–142. <https://doi.org/10.1111/j.1467-9507.1992.tb00116.x>
65. Wheatley T, Kang O, Parkinson C, Loosier CE. From mind perception to mental connection: synchrony as a mechanism for social understanding. *Soc Personal Psychol Compass.* 2012; 6: 589–606. <https://doi.org/10.1111/j.1751-9004.2012.00450.x>
66. Oullier O, Kelso JAS. Social coordination, from the perspective of Coordination Dynamics. In: Meyers RA, editor. *Encyclopedia of Complexity and Systems Science*. New York, NY: Springer New York; 2009. pp. 8198–8213. https://doi.org/10.1007/978-0-387-30440-3_486
67. Schmidt RC, Fitzpatrick P, Caron R, Mergeche J. Understanding social motor coordination. *Hum Mov Sci.* Elsevier B.V.; 2011; 30: 834–845. <https://doi.org/10.1016/j.humov.2010.05.014> PMID: 20817320
68. Sekara V, Stopczynski A, Lehmann S. Fundamental structures of dynamic social networks. *Proc Natl Acad Sci.* 2016; 113: 9977–9982. <https://doi.org/10.1073/pnas.1602803113> PMID: 27555584
69. Boiger M, Mesquita B. The construction of emotion in interactions, relationships, and cultures. *Emot Rev.* 2012; 4: 221–229. <https://doi.org/10.1177/1754073912439765>
70. Carneiro RR. On the relationship between size of population and complexity of social organization. *Southwest J Anthropol.* 1967; 23: 234–243. Available: <http://www.jstor.org/stable/3629251>
71. Changizi MA, He D. Four correlates of complex behavioral networks: differentiation, behavior, connectivity, and compartmentalization: Carving networks at their joints. *Complexity.* 2005; 10: 13–40. <https://doi.org/10.1002/cplx.20085>
72. Weng G, Bhalla US, Iyengar R. Complexity in biological signaling systems. *Science.* 1999; 284: 92–96. <https://doi.org/10.1126/science.284.5411.92> PMID: 10102825
73. Stouffer DB, Bascompte J. Compartmentalization increases food-web persistence. *Proc Natl Acad Sci.* 2011; 108: 3648–3652. <https://doi.org/10.1073/pnas.1014353108> PMID: 21307311
74. Kirschner M, Gerhart J. Evolvability. *Proc Natl Acad Sci.* 1998; 95: 8420–8427. doi:VL—95 PMID: 9671692
75. Ash J, Newth D. Optimizing complex networks for resilience against cascading failure. *Phys A Stat Mech its Appl.* 2007; 380: 673–683. <https://doi.org/10.1016/j.physa.2006.12.058>
76. Edelman GM, Gally JA. Degeneracy and complexity in biological systems. *Proc Natl Acad Sci.* 2001; 98: 13763–13768. <https://doi.org/10.1073/pnas.231499798> PMID: 11698650

77. Bar-Yam Y. Multiscale variety in complex systems. *Complexity*. 2004; 9: 37–45. <https://doi.org/10.1002/cplx.20014>
78. Sporns O. Network attributes for segregation and integration in the human brain. *Curr Opin Neurobiol*. Elsevier Ltd; 2013; 23: 162–171. <https://doi.org/10.1016/j.conb.2012.11.015> PMID: 23294553
79. Tononi GS, Sporns O, Edelman GM. A measure for brain complexity: relating functional segregation and integration in the nervous system. *Proc Natl Acad Sci*. 1994; 91: 5033–5037. <https://doi.org/10.1073/pnas.91.11.5033> PMID: 8197179
80. McPherson M, Smith-Lovin L, Cook JM. Birds of a feather: homophily in social networks. *Annu Rev Sociol*. 2001; 27: 415–444. <https://doi.org/10.1146/annurev.soc.27.1.415>
81. Moody J. Race, school integration, and friendship segregation in America. *Am J Sociol*. 2001; 107: 679–716. <https://doi.org/10.1086/338954>
82. Schelling TC. Dynamic models of segregation. *J Math Sociol*. 1971; 1: 143–186. <https://doi.org/10.1080/0022250X.1971.9989794>
83. Stark TH, Flache A. The double edge of common interest. *Sociol Educ*. 2012; 85: 179–199. <https://doi.org/10.1177/0038040711427314>
84. Blau PM. Inequality and Heterogeneity: a Primitive Theory of Social Structure. New York, NY: Free Press; 1977.
85. Kelso JAS, Engstrom DA. The Complementary Nature. MIT press; 2006.
86. Kelso JAS. Instabilities and phase transitions in human brain and behavior. *Front Hum Neurosci*. 2010; 4: 23. <https://doi.org/10.3389/fnhum.2010.00023> PMID: 20461234
87. Scheffer M, Bascompte J, Brock WA, Brovkin V, Carpenter SR, Dakos V, et al. Early-warning signals for critical transitions. *Nature*. 2009; 461: 53–59. <https://doi.org/10.1038/nature08227> PMID: 19727193
88. Wilson KG. Problems in physics with many scales of length. *Sci Am*. 1979; 241: 158–179. <https://doi.org/10.1038/scientificamerican0879-158>
89. Simon HA. The organization of complex systems. Hierarchy theory: The challenge of complex systems. 1977. pp. 245–261. https://doi.org/10.1007/978-94-010-9521-1_14
90. Schelling TC. Micromotives and Macrobbehavior. 1st ed. New York: Norton; 1978.
91. Leibold MA, Holyoak M, Mouquet N, Amarasekare P, Chase JM, Hoopes MF, et al. The metacommunity concept: a framework for multi-scale community ecology. *Ecol Lett*. 2004; 7: 601–613. <https://doi.org/10.1111/j.1461-0248.2004.00608.x>
92. Parra J, Kalitzin SN, Iriarte J, Blanes W, Velis DN, Lopes da Silva FH. Gamma-band phase clustering and photosensitivity: Is there an underlying mechanism common to photosensitive epilepsy and visual perception? *Brain*. 2003; 126: 1164–1172. <https://doi.org/10.1093/brain/awg109> PMID: 12690055
93. Tognoli E, Kelso JAS. Enlarging the scope: grasping brain complexity. *Front Syst Neurosci*. 2014; 8: 122. <https://doi.org/10.3389/fnsys.2014.00122> PMID: 25009476
94. Kelso JAS, Dumas G, Tognoli E. Outline of a general theory of behavior and brain coordination. *Neural Networks*. Elsevier Ltd; 2013; 37: 120–131. <https://doi.org/10.1016/j.neunet.2012.09.003> PMID: 23084845
95. Takamatsu A, Tanaka R, Fujii T. Hidden symmetry in chains of biological coupled oscillators. *Phys Rev Lett*. 2004; 92: 228102–1. <https://doi.org/10.1103/PhysRevLett.92.228102> PMID: 15245261
96. Yokoyama K, Yamamoto Y. Three people can synchronize as coupled oscillators during sports activities. Diedrichsen J, editor. *PLoS Comput Biol*. 2011; 7: e1002181. <https://doi.org/10.1371/journal.pcbi.1002181> PMID: 21998570
97. Kuramoto Y, Battogtokh D. Coexistence of coherence and incoherence in nonlocally coupled phase oscillators. *Nonlinear Phenom Complex Syst*. 2002; 5: 380–385. Available: <http://www.j-npcs.org/abstracts/vol2002/v5no4/v5no4p380.html>
98. Holling CS. Understanding the complexity of economic, ecological, and social systems. *Ecosystems*. 2001; 4: 390–405. <https://doi.org/10.1007/s10021-00-0101-5>
99. Kelso JAS. An essay on understanding the mind. *Ecol Psychol*. 2008; 20: 180–208. <https://doi.org/10.1080/10407410801949297> PMID: 19865611
100. Palla G, Barabási A-L, Vicsek T. Quantifying social group evolution. *Nature*. 2007; 446: 664–667. <https://doi.org/10.1038/nature05670> PMID: 17410175
101. Wang J, Suri S, Watts DJ. Cooperation and assortativity with dynamic partner updating. *Proc Natl Acad Sci*. 2012; 109: 14363–14368. <https://doi.org/10.1073/pnas.1120867109> PMID: 22904193

102. Haken H, Peper CE, Beek PJ, Daffertshofer A. A model for phase transitions in human hand movements during multifrequency tapping. *Phys D Nonlinear Phenom.* 1996; 90: 179–196. [https://doi.org/10.1016/0167-2789\(95\)00235-9](https://doi.org/10.1016/0167-2789(95)00235-9)
103. Arnold VI. Small denominators. I. Mapping of the circumference onto itself. *Collected Works.* Berlin, Heidelberg: Springer Berlin Heidelberg; 2009. pp. 152–223. https://doi.org/10.1007/978-3-642-01742-1_10
104. Jensen O, Colgin LL. Cross-frequency coupling between neuronal oscillations. *Trends Cogn Sci.* 2007; 11: 267–269. <https://doi.org/10.1016/j.tics.2007.05.003> PMID: 17548233
105. Lemke JL. Across the scales of time: artifacts, activities, and meanings in ecosocial systems. *Mind, Cult Act.* 2000; 7: 273–290. https://doi.org/10.1207/S15327884MCA0704_03

S1. Supporting information

Re: “Critical diversity: divided or united states of social coordination” by Zhang et al.

Section A-Section D detail the main data processing techniques and statistical methods involved in the main text. Section A describes the computation of phase, relative phase (ϕ), phase-locking value (*PLV*), instantaneous frequency and frequency ratio (*FR*). Section B shows the statistical method for comparing the level of phase-locking (Fig 4A). Section C explains how linear regression was used to assess the level of integration and how to compute critical diversity (Fig 4B). Section D describes how to construct the confidence interval for null distributions in Fig E (corresponding to Fig 2) and Fig 3.

Section E-Section L show supplementary results to those reported in the main text. Section E shows that participants were able to tap at the required frequency according to instructions. Section F shows how episodes of strong interaction were extracted from relative phase time series, and shows distributions of the duration and phase patterns in those episodes. Section G shows statistical comparisons of the relative phase distributions in Fig 2 to chance level distributions. Section H shows statistically how dyadic phase relations can be influenced by chances in its surrounding network structure. Section I provides additional discussion on metastable dynamics in multiagent coordination complementing Fig 1 and Fig 5. Section J presents a method to quantify metastability (metastable index), the validation of the method with simulated data, and results obtained from the present experimental data. Section K shows how simulated data used in Section J were obtained. Section L shows the main effects corresponding to the interaction effects shown in Fig 4A.

Section A. Preprocessing of recorded signals

In the current study, we characterize social coordination in terms of frequency and phase relations. Here we detail how frequency and phase related variables were transformed from raw signals (square waves consisting of zeros and ones, see Experimental Setup). We define the inter-tap interval (ITI) as the time

difference between the onsets of two consecutive taps. Instantaneous Frequency (F) is the reciprocal of ITI, interpolated linearly between taps in accord with the original sampling rate (250Hz). We obtained Phase (θ_i) by first assigning the value $2\pi(n - 1)$ to the onset of the n^{th} tap of the i^{th} individual, and then interpolating samples in between with a cubic spline method. Further, we define relational variables Frequency Ratio (FR_{ij}) and Relative Phase (ϕ_{ij}) between individual i and j as

$$FR_{ij} = \frac{\min(F_i, F_j)}{\max(F_i, F_j)}$$

and

$$\phi_{ij} = \theta_i - \theta_j$$

respectively.

To quantify the degree of phase coordination, we segment each time series into consecutive 3s windows, and calculate the Phase-Locking Value (PLV) within such windows.

$$PLV = 1 - CV = \frac{1}{N} \left| \sum_{n=1}^N e^{i\phi[n]} \right|$$

where CV is circular variance, and N is the total number of samples in a window (750 pts). PLV ranges from zero to one. A value of one indicates the maximal degree of coordination, and a value of zero indicates no coordination.

Section B. Multivariate analysis of variance (MANOVA)

To study how dyadic coordination within and between initial groups (denoted as variable “relation” with two categories: “within-group” and “between-group”) changes as diversity varies (i.e. between-group difference in frequency predispositions, $\delta f = 0, 0.3, 0.6$ Hz), we performed a 2×3 (relation \times δf) MANOVA to compare the mean PLV in different conditions, using Type III Sums of Squares. Multiple comparisons were performed using Tukey HSD (honest significant difference) tests.

Section C. Linear regressions and critical frequency identification

To study the macro organization of groups, we examined the relation between within-group and between-group phase coordination, and how it changes as diversity (δf) increases. Least Square method was used to obtain the regression line for each δf ,

$$PLV_{between-group}^{\delta f} = \beta_0^{\delta f} + \beta_1^{\delta f} PLV_{within-group}^{\delta f} + \epsilon^{\delta f}$$

The slope $\beta_1 = \beta_1^{\delta f}$ is the relation between within- and between-group coordination, an index of the degree of integration between two initial groups. If $\beta_1 = 1$, there is only one undifferentiated supergroup. $0 < \beta_1 < 1$ indicates that initial groups integrated into a supergroup but there is remnant of the diversity (coordination with one group increases the coordination with the other group but not as much as when there is no diversity). $\beta_1 < 0$ indicates that initial groups remain segregated (coordination with one group decreases coordination with another group).

If there exists a diversity δf such that within-group coordination does not vary with between-group coordination (degree of integration $\beta_1^{\delta f} = 0$), we call it a critical diversity (δf^*) - a separatrix between regimes of integration and segregation of two initial groups. To obtain δf^* , we regressed the degree of integration β_1 against diversity δf ,

$$\beta_1 = \alpha_0 + \alpha_1 \delta f + \varepsilon$$

and estimated where the regression line crosses $\beta_1 = 0$,

$$\delta f^* := -\frac{\alpha_0}{\alpha_1}$$

Section D. Distributional comparison

To verify how much the distribution of relational variables (FR , ϕ) in each condition reflects genuine coordination, we constructed chance level distributions by random permutations of all taps within each condition (i.e. taps produced following the same metronome). A total of 10,000 random permutations were performed. For each permutation, relational variables were computed following the same procedures as that of the original data (see Section A) and a probability density function (PDF) was computed for each variable using a 100-bin histogram. Given a significance level of $p=0.0005$ for each bin (based on Bonferroni correction for $\hat{p}=0.05$ for the entire distribution), we computed the confidence interval around chance level distribution (two-tailed) as between $(100 - 50p)$ percentile and $50p$ percentile of the 10,000 random distributions for each bin. The real distribution is significantly different from chance at a specific value of FR or ϕ , if the probability density of this value is outside the confidence interval (seen as light-colored bands in main text Figs).

Section E. Participants tapped at (near) metronome frequencies as per instruction

Overall, participants followed instructions to tap at the metronome frequencies both during pacing (Fig A, top) and interaction (Fig A, bottom). On average, participants tapped a little faster than the metronome: by 0.074 ± 0.41 Hz during pacing ($t(2070)=8.26$, $p<0.001$) and 0.14 ± 0.45 Hz during interaction ($t(2071)=14.35$, $p<0.001$).

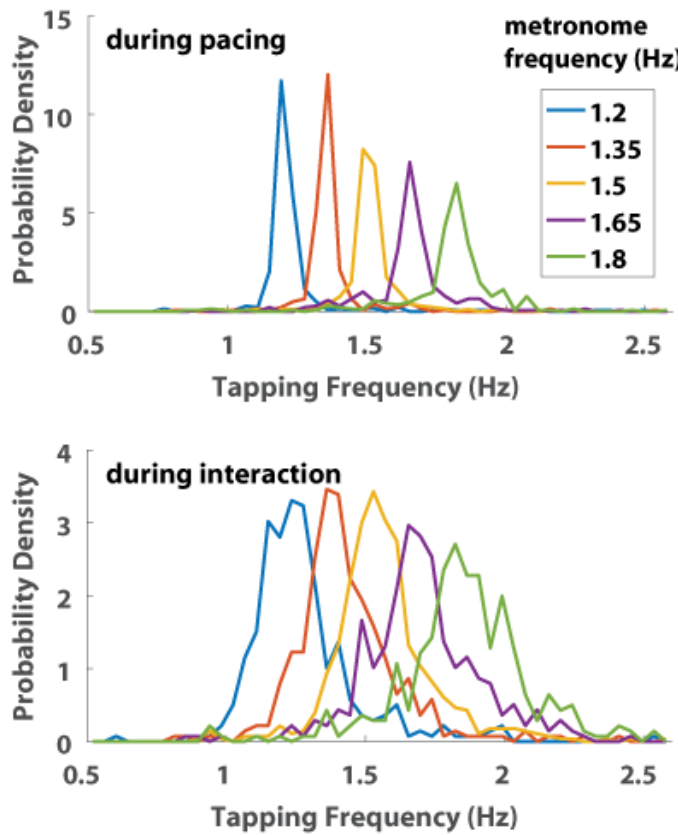


Fig A. Distributions of tapping frequency during pacing (top panel) and during interaction (bottom panel). Five Probability density functions of participants' tapping frequency are shown for five different metronome frequencies (1.5 Hz for $\delta f=0$ Hz, 1.35 and 1.65Hz for $\delta f=0.3$ Hz, 1.2 and 1.8Hz for $\delta f=0.6$ Hz).

Section F. Episodes of strong phase coordination

To identify strongly attractive phase patterns and their persistence, an expert trained in coordination dynamics manually extracted the onsets and offsets of strong phase coordination (i.e. periods of constant phase relations with small fluctuation) in time series of dyadic relative phase. One relative phase time series was presented at a time and in random order. The inspector was blind from phase relations other than the one under inspection and the condition (i.e. δf) from which a time series was extracted.

The distribution of the duration of manually extracted episodes of strong coordination (Fig) shows that phase coordination primarily occurred for short periods (<10s); long lasting ones (stable phase locking) also appeared, but the occurrence was very rare.

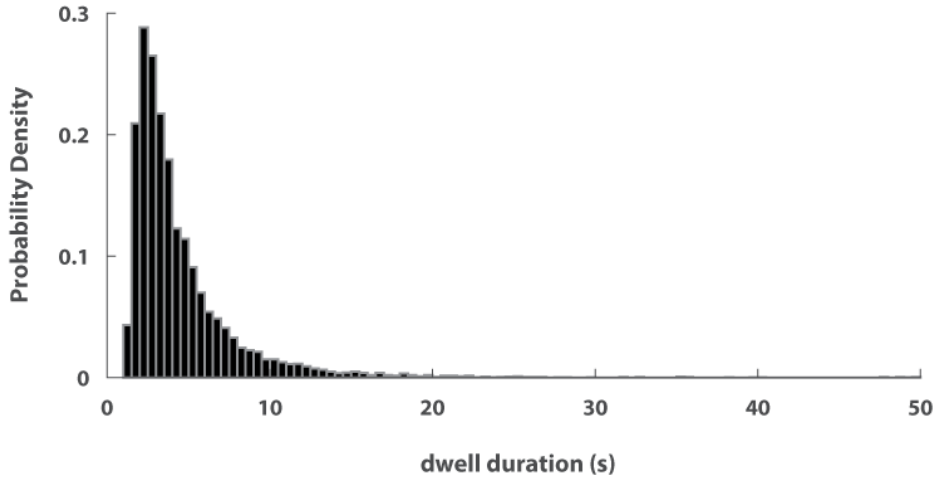


Fig B. Distribution of the durations of strong phase coordination.

Fig C shows the distributions of relative phase within those episodes of strong interaction. Within groups (Fig C(A)), both inphase (peak near $\phi = 0$) and antiphase (smaller peak near $\phi = \pm\pi$) are dominant phase patterns with inphase stronger than antiphase, regardless of diversity conditions (color). Between groups (Fig C(B)), the dominance of inphase pattern was retained across different levels of diversity, but antiphase gradually lost its attraction with increasing diversity (gradually flattened peaks near $\phi = \pm\pi$ from blue to red to yellow).

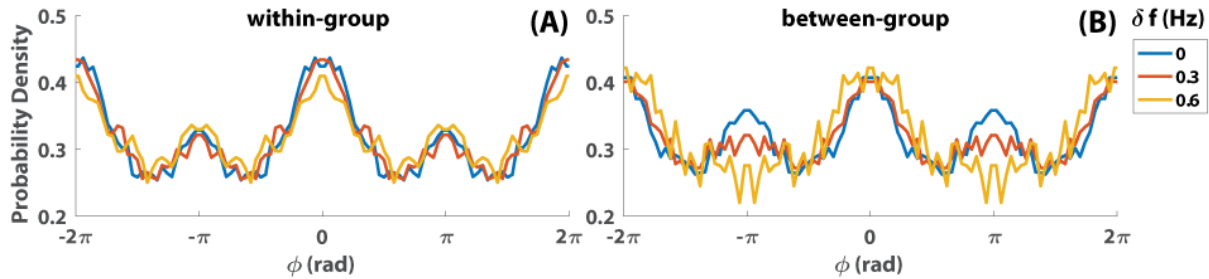


Fig C. Relative phase distribution during strong coordination for within-group dyads (A) and between-group dyads (B).

To see whether the relative phase relation was affected by the number of partners one simultaneously coordinated to, we computed for each agent the number of people he/she simultaneously engaged in strong interaction with (i.e. number of connections, the horizontal axis in Fig D) and the corresponding relative phase patterns adopted. We were particularly interested in the dominance of near inphase (i.e. $|\phi| < \pi/3$) and near antiphase ($|\phi| > 2\pi/3$) patterns (Fig D, blue, red respectively), for which we computed the probability density for each fixed number of connections (1 to 6; the maximal number connections one can make is 7, but its very rare occurrence made for an unreliable estimate, thus not shown). We found that the dominance of near inphase patterns gradually increased as one connected to more individuals; in contrast, the dominance of near antiphase patterns was steady across a small number of connections ($N \leq 4$) then gradually declined for a higher number of connections. This finding suggests that inphase, as the most symmetric form of phase pattern, may serve as a scaffold for individuals to simultaneously coordinate with multiple people (as in a rowing eight, for instance).

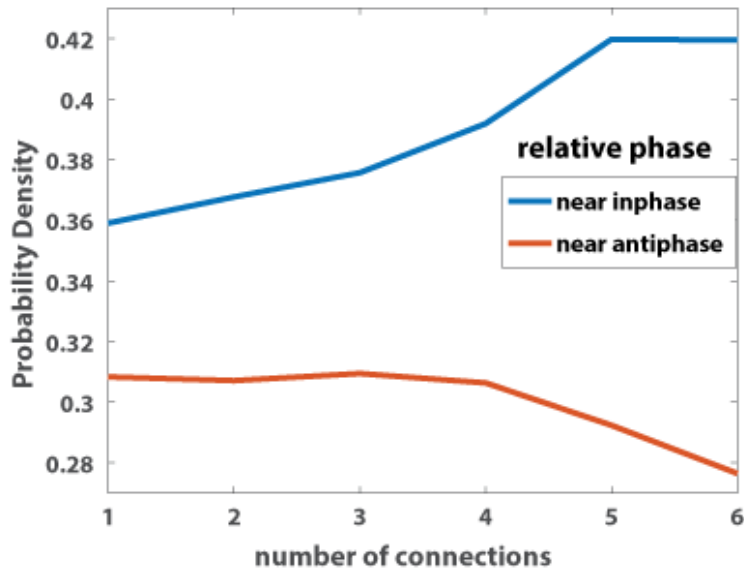


Fig D. Dominance of near-inphase vs. near-antiphase patterns as a function of the number of connections.

Blue line indicates the probability density of near inphase patterns ($|\phi| < \pi/3$) when participants simultaneously coordinated with different numbers of people (i.e. number of connections); red line indicates near-antiphase patterns ($|\phi| > 2\pi/3$). The trend of lines show how the dominance of near-inphase and near-antiphase patterns change with increasing number of connections: inphase was increasingly preferred whereas antiphase diminished for connection number exceeding 4.

Section G. Relative phase distributions compared to chance level

To identify which patterns of phase coordination were significantly above chance level, confidence intervals (two-sided, for $\hat{p} < 0.05$, where ‘hat’ denotes Bonferroni correction for multiple comparison in 100 bins of an entire distribution) were computed from randomly permuted data (as detailed in Section D), and are shown as light-color bands in Fig E. A black bar marks wherever the real distribution is outside the confidence interval for three consecutive bins out of the hundred bins that make up the histogram. Within-group phase coordination shows significantly more near inphase patterns ($\phi \approx 0$) than chance levels ($\hat{p} < 0.05$, for 0 to 0.24π , Fig E(A1)), while between-group coordination, though with a hint

of inphase preference, was barely above chance ($\hat{p} < 0.05$, for 0.05π to 0.08π , Fig E(A2)). For low diversity ($\delta f=0$, 0.3 Hz, Fig E(B1-2)), the probability density near inphase was significantly above chance (highest peaks in blue and red curves). As diversity increased, the attractiveness of inphase patterns diminished, and beyond the critical diversity level ($\delta f^*=0.5$ Hz) its statistical significance eventually vanished ($\delta f=0.6$ Hz, Fig E(B3)).

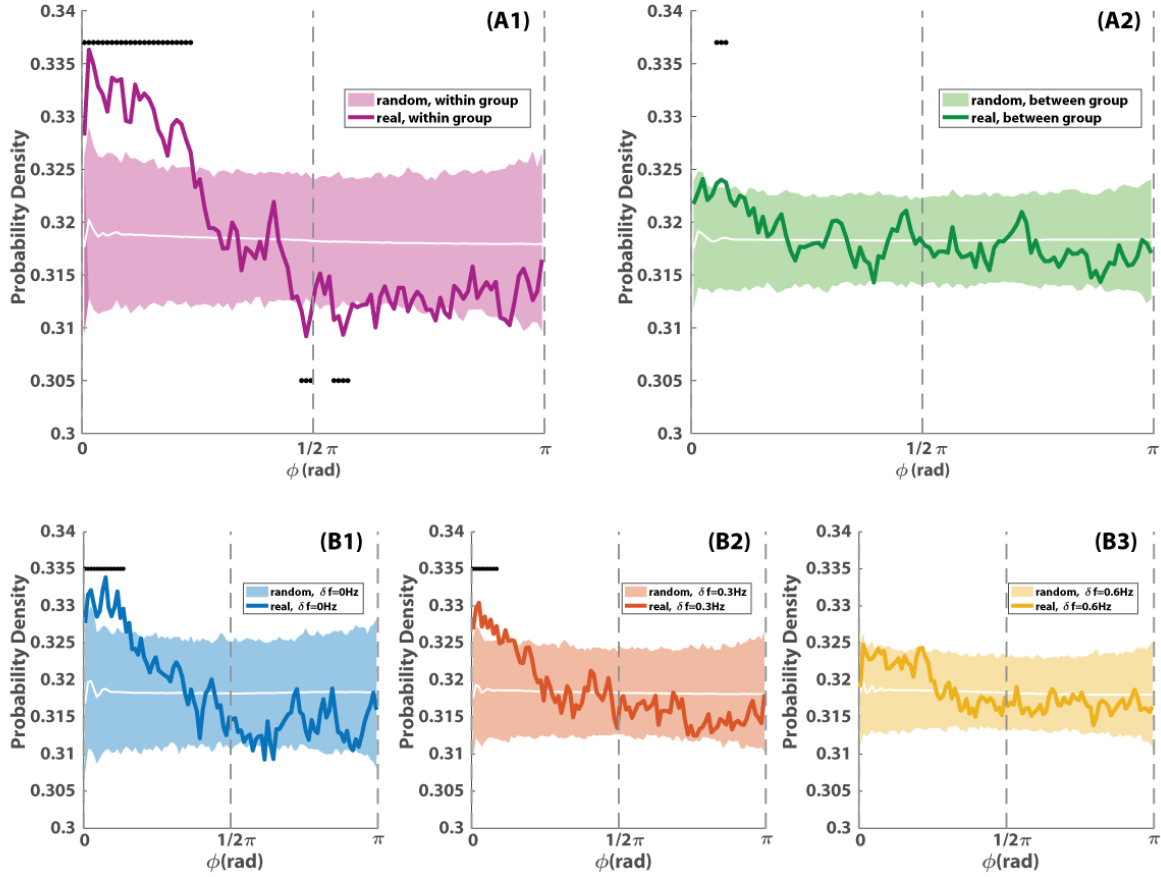


Fig E. Distributions of relative phase with respect to chance level. Within-group phase coordination (A1) shows more patterns near inphase are significantly above chance than between-group coordination (A2). At the aggregate level of ensembles, a tendency for inphase coordination is observed (B1-B3, solid lines), which is significantly different from chance (shaded areas) for lower diversity levels (B1, B2; black bar above indicates where more than 3 consecutive bins reached significance level $\hat{p} < 0.05$).

Section H. Phase relations are subject to internal and external changes in network structure

Using the onset and offset of each episode of strong coordination (as in Section F), we constructed a series of networks (i.e. graphs) representing the evolution of an ensemble's coordinative behavior during each trial of interaction (graphic examples see Fig 1A3, B4 and Fig 5D). Each node of a network represents a participant and an edge exists between two nodes if and only if the two participants are strongly coordinated at the time. Thus, we were able to detect changes in the coordinative structure or network (i.e. any two persons in the ensemble who were coordinated become uncoordinated or vice-versa) and to determine how dyadic relative phase was influenced by such changes. Fig F(A) shows distributions of the shift in dyadic relative phase between consecutive 2s windows: the blue curve depicts phase shifts in strongly coordinated dyads when there was no change in network (baseline; blue); the red curve depicts how much relative phase shifted in strongly coordinated dyads when other relations (edges) were forming or breaking up in the network (i.e. changes external to the dyad of interest; orange); and the yellow curve depicts how much phase shift occurred in dyads who were entering or leaving a strong coordination themselves (i.e. changes internal to the dyad of interest; yellow). Based on ANOVA, significant differences were found between the three conditions (Fig F(B); $F(2,663)=1165.33$, $p<0.001$). Relative phase shifted the most when the dyads themselves were changing from being coordinated (dwell) to uncoordinated (escape) or vice-versa (yellow; greater than blue and red, $p<0.001$, based on Tukey HSD). For strongly coordinated dyads (red), the phase relation was also shifted by changes elsewhere in the network to an extent significantly greater than baseline (i.e. no change in the network, blue; $p<0.001$, Tukey HSD). This result demonstrates quantitatively that dyadic coordination dynamics was influenced by the multiagent environment in which it is embedded.

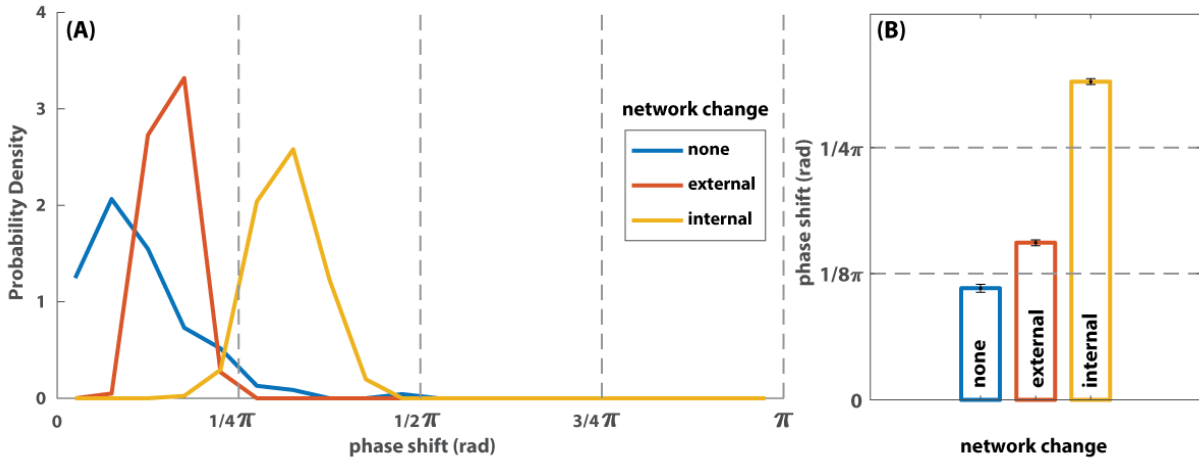


Fig F. Phase shift induced by internal and external changes of network structure. (A) Distribution of phase shift between consecutive 2s windows in dyads with strong relations: when (blue) there is no change in the network (all dyads un/coordinated remained un/coordinated), (red) the strongly coordinated dyad remained coordinated but changes occurred elsewhere in the network, and (yellow) the strongly coordinated dyad changed from being coordinated to uncoordinated or vice-versa. (B) compares the mean of distributions shown in (A) where error bars indicate the standard error of the mean. When there is a change in the network structure, both the dyads that remained coordinated and those that became (un)coordinated underwent a shift in relative phase significantly greater than baseline (i.e. when there was no change in the network structure, blue; all $p<0.001$), but the former experienced a smaller shift than the latter (red, yellow respectively; $p<0.001$).

Section I. Metastability in the multiagent environment

As exemplified in Fig 1 of the main text, participants engaged in metastable phase coordination.

Metastably coordinated agents intermittently dwell at and escape from certain preferred phase patterns (i.e. coexistence of integration and segregation at dyadic level), which can lead to constant spatial reorganization (e.g. Fig 1, A3 and B4, Fig 5) as a flexible form of within-group integration. Here we want to emphasize that such spatial organization and reorganization is inseparable from the group's frequency organization. The time scale of a metastable relation between two agents depends on the difference between their natural frequencies (or frequency predispositions) – the greater the difference, the shorter and more recurrent the dwells (Tognoli and Kelso 2014). For example, in the trial illustrated in Fig 1B,

we showed that the shortest and most recurrent dwells in a group of four occurred between agents 4 and 3 (B1, blue). In Fig G, we show the corresponding frequency trajectories of these four agents. Notice that agent 3 (Fig. G, orange) tapped at a much higher frequency, on average, than the rest of the group; in contrast, agents 1, 2, 4 were much closer with each other in frequency, and their phase dwells lived on a longer time scale (Fig 1, B3, red and green). Furthermore, metastable phase coordination is accompanied by corresponding oscillations in instantaneous frequency: for a pair of agents to escape from a phase pattern, at least one of them must accelerate/decelerate to leave the common frequency, and for a pair to dwell in a particular phase pattern, two agents each at a distinct frequency must temporally accelerate/decelerate to converge to the same frequency (this property is used for a statistical analysis of metastability in Section J). This can be clearly seen in Fig G: agent 3 (orange) exhibited the most pronounced and rapid frequency oscillation, less so for agent 4 (yellow), and even less for agents 1 and 2 (red and pink). This is in stark contrast with the idealized picture of conventional synchronization where agents converge to and stick with the same frequency to maintain constant phase relations. Thus, metastability not only afford an overall integrated group flexible spatial organization but also preserve its frequency diversity – two sides of the same coin.

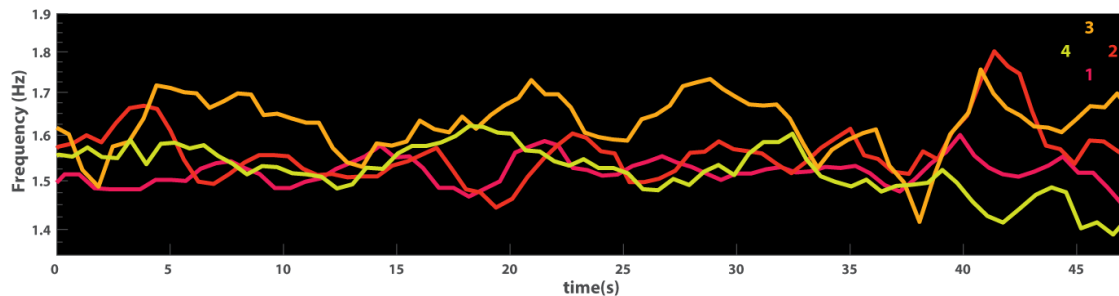


Fig G. Frequency variation in a group of metastably coordinated agents. This Fig shows instantaneous frequencies of agents whose phase coordination was illustrated in Fig 1B. The time series were smoothed with a 4-point moving average to capture the dynamics that best reveals spatial reorganization. Agent 3 had the highest tapping frequency, which oscillated up and down to join other agents at different times (e.g. around 17s, 25s and 33s), corresponding to the dwells illustrated in Fig 1B for relative phase between 3 and 4. Agent 4 oscillated between coordinating with 3 or 1-2, reflected in Fig 1B as short dwells in trajectories 1-4

and 4-3. Agents 1 and 2 were at the same frequency most of the time, reflected as the long dwell of 1-2 in Fig 1B.

The above case (Fig G) shows how a small group maintains long-term integration through constant transformation, but this may not be as easy for a larger group. Fig H(A,B) shows an example of eight-agent interaction where all agents were predisposed to the same frequency: A shows agents' frequency trajectories, and B shows the dynamics of their spatial organization as grouping dynamics (each column depicts which agents were phase coordinated as a group at a particular time, where agents in the same group were labeled with the same color; here “group” is equivalent to connected component in network structure). Early on in the trial, the ensemble of eight dwelled at very similar frequencies, although with constantly changing spatial configuration. This, however, did not last long as around 10-15s the big group began to diverge in frequency (Fig H(A)) and broke up into smaller, but more sustainable groups (e.g. pink and blue groups in Fig H(B)). This example demonstrates that when diversity is low, each agent has many potential partners to coordinate with: such potential relations may compete with each other, resulting in rapid switching between different partners and a lack of persistent spatiotemporal organization. To achieve more persistent grouping patterns, agents may diverge in their frequencies hence providing some separation protecting local structures. This example complements the high diversity case reported in the main text (Fig 5) in which spatial organization was much more persistent but not without sudden transitions – ensembles with high initial diversity had sufficient divergence to begin with. The grouping dynamics corresponding to Fig 5 is shown in Fig H(C) for visual comparison, in which the spatial organization is much more ordered and better sustained.

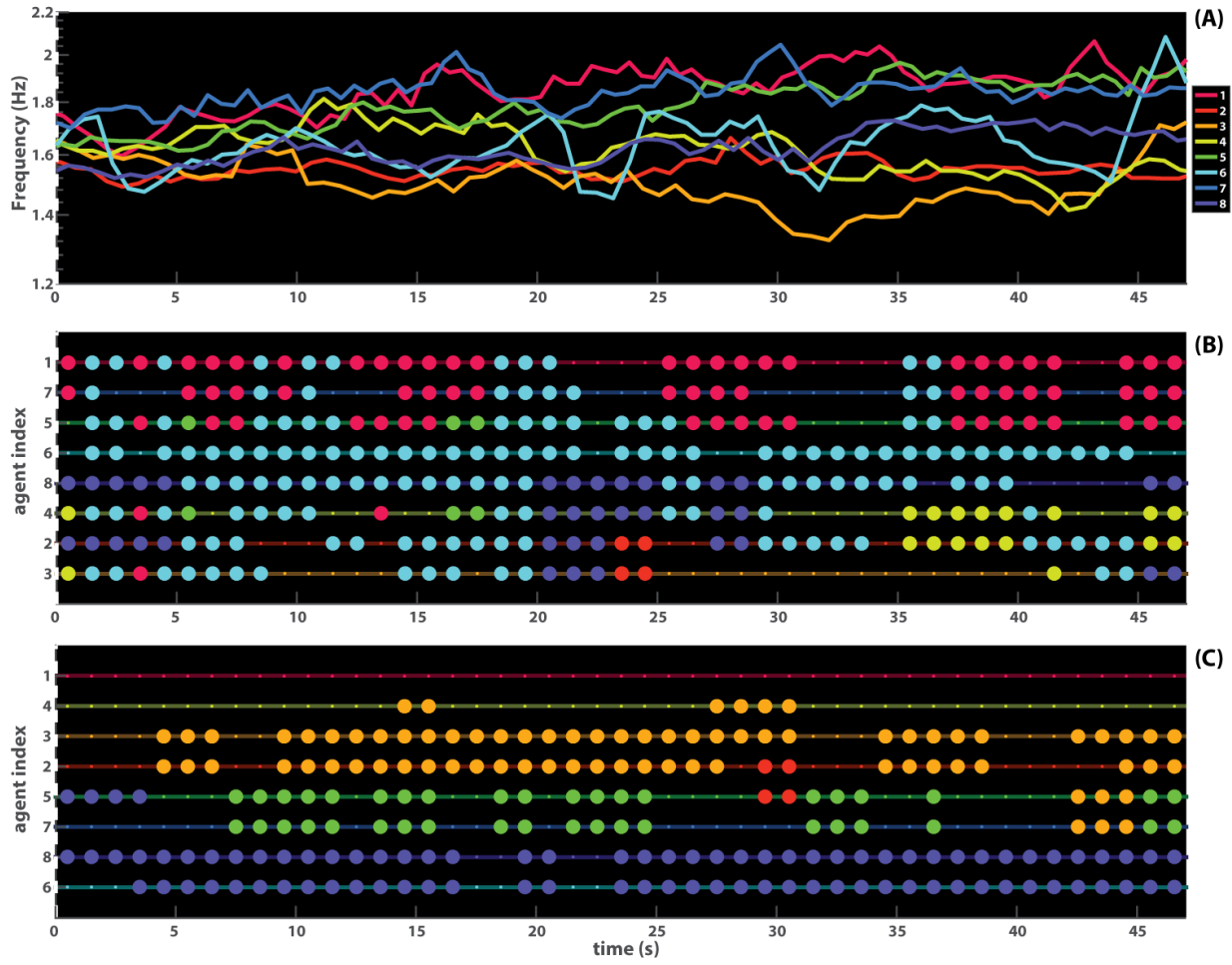


Fig H. Evolution of coordination dynamics among eight agents with low diversity (A-B) vs. high diversity (C).

(A) Instantaneous frequencies of eight agents who were all paced with the same metronome. The frequency dispersion among agents gradually increased over the course of interaction. By the end of the trials, agents diverged into smaller groups. (B) Grouping dynamics among the eight agents with low initial diversity corresponding to (A). Each color represents a particular group, in which all members of the group were directly or indirectly connected through strong phase coordination as identified in Section F. Each row represents one agent whose group affiliation was denoted by the color of the circle (no circle means the agent was by him/her self), arranged, from top to bottom, from highest to lowest average frequency. The grouping (spatial configuration) changes rapidly early on in the trial but gradually forms a more stable structure later in the trial (agents are attracted to a three-group organization: 1-7-5, 6-8, and 4-2; see text). (C) For comparison, grouping dynamics among the eight agents with high initial diversity, corresponding to the example in Fig 5. The grouping (three groups/dyads: 3-2, 5-7, and 8-6) remained prevalent throughout the

interaction, but not without occasional reorganization, e.g. around 30s (see main text for details). That is, initial separation in frequency seem to favor the sustenance of lasting coordinative structures as in C, whereas initial similarity might create incidental opportunities for interaction that constantly perturb ongoing coordinative structures (A-B).

Section J. Quantification of metastability for statistical analysis

As discussed in Section I, metastable coordination entails fluctuations in agents' instantaneous frequency (e.g. Fig G, agent 3). If a phase relation between two agents is metastable, then as the relative phase (ϕ) goes through 2π (wrapping back to the same phase relation), there should be correspondingly oscillations in the relative frequency between the two agents (or equivalently oscillations in the derivative of ϕ). The degree of metastability was assessed based on this relation between the number of times ϕ wrapped through 2π (called the winding number), and the number of oscillations in relative frequency. We define a metastable index (MI) as

$$MI = P[\Delta F_{ij}] \left(\frac{wind(\phi_{ij})}{T} \right) \quad \text{Eq.2}$$

where $\Delta F_{ij} = F_i - F_j$ is the relative frequency between participant i and j (normalized to Euclidean norm 1, mean removed, with an added small value $\epsilon = 10^{-4}$ Hz, explained later), $P[\Delta F_{ij}]$ is the power spectrum of ΔF_{ij} (in Decibels, dB), $wind(\phi_{ij}) := \frac{|\phi(T) - \phi(0)|}{2\pi}$ is the winding number, ϕ is the unwrapped relative phase and T is the length of the trial. This metric thus reflects the interplay between frequency fluctuation and phase wrapping in metastable relations. MI is high when metastable coordination is strong with a pronounced alternation of dwells and escape times (for each cycle of phase wrapping there is a corresponding oscillation of frequency difference), but low when the coordination is very weak (faint dwell/escape approaching uncoupled oscillators) or completely stable (thus not metastable). Completely stable phase-coordination corresponds to $P[\Delta F_{ij}](0)$ (i.e. no phase wrapping) which also corresponds to

the mean of ΔF_{ij} , thus we set mean of ΔF_{ij} to be ϵ so that in the power spectrum we have $P[\Delta F_{ij}](0) \approx -40dB$ (here ϵ must be non-zero, otherwise $P[\Delta F_{ij}](0) \rightarrow -\infty$).

To test whether MI truly reflects metastable coordination, we first validate MI with simulated data of dyadic coordination based on a well-tested theoretical model (extended HKB; see Section K for details). Based on existing empirical and theoretical studies of metastable coordination dynamics (Kelso, 1995; Tognoli and Kelso, 2014), we expect metastability to be high for weak/moderate coupling between agents with sufficiently large diversity in their frequency predispositions, and to be minimal when two agents do not couple to each other or are completely phase-locked to each other. Complete phase-locking results from a combination of strong coupling and low diversity. Were MI a valid metric, we should see a decrease of metastability with increasing coupling strength. First, 600 trials were simulated for dyads with zero coupling ($a=0, b=0$, thus no coordination), three levels of intrinsic frequency difference (i.e. diversity, $\delta f=0, 0.3, 0.6$ Hz, 200 trials for each level) and random initial conditions. Without coupling, the resulting MIs were -40.97 ± 2.10 dB for all three levels of diversity – the minimal level of metastability as expected. Further, 1800 trials ($200 \times 3 \times 3$) were simulated for dyads with three levels of coupling ($b=0.1, 0.4$, or 0.8 , with fixed $a=1$), three levels of diversity (mean $\delta f=0, 0.3, 0.6$ Hz, with 0.1 Hz variance), and random initial conditions. The parameters (black circles in Fig I) were so chosen to span the boundary between stable and metastable regimes of the model used to simulate coordination (yellow vs. blue areas in Fig I; see Section K for details).

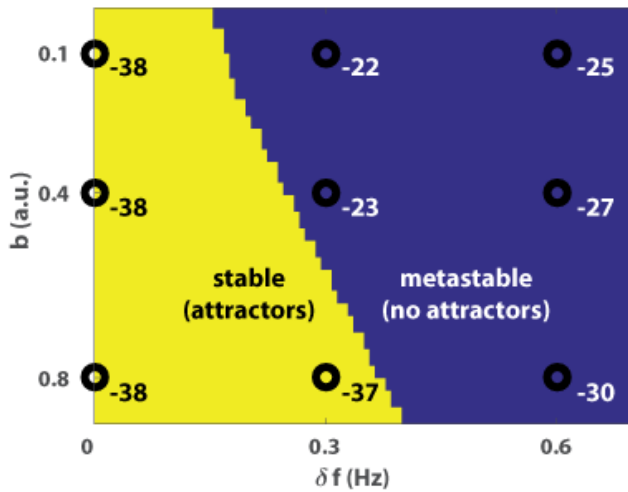


Fig I. Parameter space of the theoretical model used for simulation (extended Haken-Kelso-Bunz equations, Kelso et al, 1990, also see Section K). Vertical axis represents the coupling strength b and horizontal axis the frequency difference between two oscillatory components. Yellow area is the stable regime where there is at least one attractor of the system; blue area is the metastable regime where there is no attractor but attracting tendencies near certain phase patterns remain, giving rise to intermittent coordination (dwells and escapes). Black circles are parameter values chosen for the validation of MI. The number next to the circle indicates the average MI of simulated data based on that set of parameter values. MI successfully reflects the stable vs. metastable nature of the simulated coordination: near -40 dB in stable regime (yellow area) and between -30 to -20 dB (far from -40 dB) in metastable regime (blue).

From the simulated data, we found that, overall, MI decreased monotonically with increasing coupling strength (for $b=0.1, 0.4$, and 0.8 , the MIs are -28.43 ± 0.23 dB, -29.92 ± 0.23 dB, and -35.07 ± 0.23 dB respectively, not shown in Fig; MANOVA main effect, $F(2,1971)=229.79$, $p<0.0001$; post hoc test with Tukey HSD, all $p<0.0001$); and MI is the lowest for $\delta f=0$ Hz (-38.19 ± 0.23 dB, not shown, main effect, $F(2,1791)=707.63$, $p<0.0001$; post hoc test, greater than for $\delta f=0.3, 0.6$ Hz, both $p<0.0001$), while MI for $\delta f=0.3$ and 0.6 Hz were not significantly different from each other (-27.78 ± 0.23 dB and -27.44 ± 0.23 dB respectively, not shown, post hoc test, $p>0.05$). A breakdown of all conditions is shown in Fig J(B) (MANOVA, interaction effect, $F(4,1791)=108.43$, $p<0.001$). For weak coupling ($b=0.1, 0.4$), metastability was greatest when diversity was moderate ($\delta f=0.3$ Hz, orange); slightly lowered when

diversity became too high ($\delta f=0.6$ Hz, yellow), but dropped close to minimum for low diversity ($\delta f=0$ Hz, blue). When the coupling is strong ($b=0.8$), dyads with moderate diversity also lost metastability, indicating complete phase-locking. As expected from existing studies of metastability weak coupling and moderate diversity led to greater MI while strong coupling diminished MI, thereby showing MI is a valid metric of metastability.

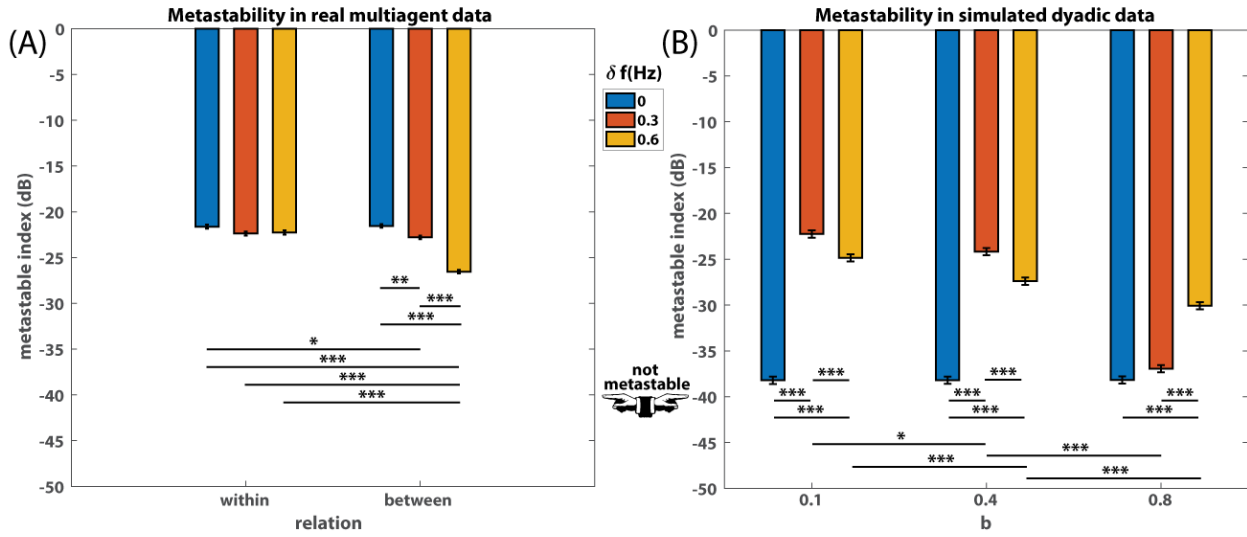


Fig J. Metastable coordination within and between groups. (A) Metastability in real data collected in the present experiment. (B) Metastability in simulated data of dyadic coordination. (* p<0.05; ** p<0.01; *p<0.001)**

Applying MI to the actual data of the present experiment, we found main effects (not shown in Fig) for both grouping relation (whether metastable coordination occurs within- or between-group, $F(1,7246)=77.67$, $p<0.0001$) and diversity δf ($F(2,7246)=89.21$, $p<0.0001$): within-group coordination ($MI=-22.09\pm0.13$ dB) exhibits greater metastability than between group (-23.63 ± 0.11 dB; post hoc test, Tukey HSD, $p<0.0001$), and the metastable index monotonically decreases with increasing diversity (for $\delta f=0$ Hz, -21.58 ± 0.15 dB, for $\delta f=0.3$ Hz, -22.58 ± 0.15 dB, and for $\delta f=0.6$ Hz, -24.40 ± 0.15 dB; post hoc test, all $p<0.0001$). MI was far from the minimal value (≈ -40 dB) in every condition. This indicates that the phase coordination present in this experiment is overwhelmingly metastable. A significant interaction

effect between grouping relation and diversity was also found ($F(2,7246)=62.39$, $p<0.0001$) as shown in Fig J(A). There was no significant change in the level of metastability for within-group coordination with increasing intergroup difference (post hoc test, $p>0.05$; Fig J(A), left), nor was any within-group metastability significantly different from between-group metastability when diversity was minimal ($\delta f=0$ Hz, Fig J(A), right, blue bar; $p>0.05$). With increasing diversity ($\delta f=0.3$, 0.6 Hz, Fig J(A), right, orange and yellow bars), metastability in between-group coordination decreases (though still far from minimum - 40 dB). Overall, these results suggest that in this experiment metastable relations, rather than stable ones, are the building blocks of spontaneous multiagent coordination, even in the case of lowest diversity ($\delta f=0$ Hz).

Section K. Simulations of dyadic interaction

Dyadic rhythmic coordination has been extensively studied in existing research (see main text). The extended Haken-Kelso-Bunz equation (Fuchs et al 1996; Kelso, et al., 1990) is a well-tested model that captures the essential dynamics of dyadic coordination:

$$\dot{\phi} = \Delta\omega - a \sin \phi - 2b \sin 2\phi \quad \text{Eq. 1}$$

where ϕ is the relative phase between two oscillators, $\dot{\phi}$ is the rate of change of relative phase, $\Delta\omega$ is the difference between the two oscillators' natural frequency, and the ratio b/a reflects the coupling strength. Numeric solutions (2400 simulated 50s trials) were obtained using MATLAB (ode45), which were used to validate Metastable Index (MI, for details see Section J) and to produce results shown in Fig J(B).

Section L. Main effects of experimental conditions on phase-locking

Overall, within-group dyads exhibited greater phase-locking than between-group dyads (main effect, $F(1,7246)=604.7$, $p<0.001$); diversity (δf) weakened phase-locking (main effect, $F(1,7246)=338.6$; post hoc test, all $p<0.001$).

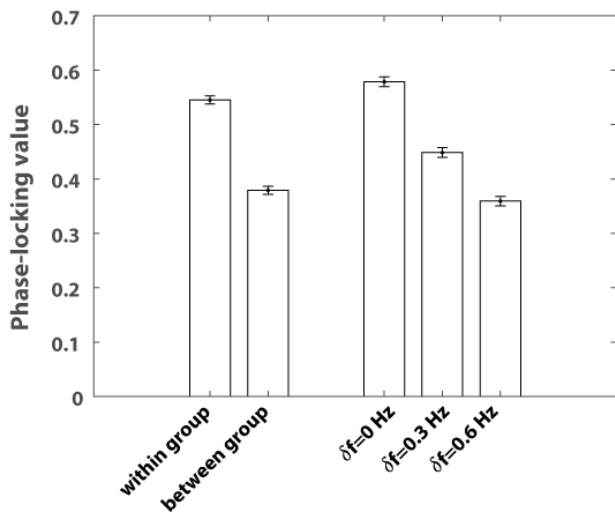


Fig K. Main effects of grouping relation (left cluster) and intergroup difference (right cluster) on phase coordination in MANOVA.

SI References

- Fuchs, A., Jirsa, V. K., Haken, H., & Kelso, J. A. S. (1996). Extending the HKB model of coordinated movement to oscillators with different eigenfrequencies. *Biological Cybernetics*, 74(1), 21–30. <https://doi.org/10.1007/BF00199134>
- Kelso, J. A. S., Del Colle, J. D., & Schöner, G. (1990). Action-perception as a pattern formation process. In M. Jeannerod (Ed), *Attention and performance 13: Motor representation and control* (Vol. 45, pp. 139–169). Hillsdale, NJ, US: Lawrence Erlbaum Associates, Inc.
- Tognoli, E., & Kelso, J. A. S. (2014). The metastable brain. *Neuron*, 81(1), 35–48. <https://doi.org/10.1016/j.neuron.2013.12.022>